MODEL EQUATIONS AND INSTABILITY REGIONS FOR THE SEDIMENTATION OF POLYDISPERSE SUSPENSIONS OF SPHERES

RAIMUND BÜRGER[A,*], KENNETH HVISTENDAHL KARLSEN[B], ELMER M. TORY[C], AND WOLFGANG L. WENDLAND[A]

ABSTRACT. The one-dimensional kinematical sedimentation theory for suspensions of small spheres of equal size and density is generalized to polydisperse suspensions and several space dimensions. The resulting mathematical model, obtained by introducing constitutive assumptions and performing a dimensional analysis, is a system of first-order conservation laws for the concentrations of the solids species coupled to a variant of the Stokes system for incompressible flow describing the mixture. Various flux density vectors for the first-order system have been proposed in the literature. Some of them cause the first-order system of conservation laws to be non-hyperbolic, or to be of mixed hyperbolic-elliptic type in the bidisperse case. The criterion for ellipticity is equivalent to a well-known instability criterion predicting phenomena like blobs and viscous fingering in bidisperse sedimentation. We show that loss of hyperbolicity, that is the occurrence of complex eigenvalues of the Jacobian of the first-order system, can be viewed as an instability criterion for arbitrary polydisperse suspensions, and that for tridisperse mixtures this criterion can be evaluated by a convenient calculation of a discriminant. We determine instability regions (or alternatively prove stability) for three different choices of the flux vector of the first-order system of conservation laws. Consequently, mixed or non-hyperbolic, rather than hyperbolic, systems of conservation laws are the appropriate general mathematical framework for polydisperse sedimentation. The stability analysis examines a first-order system of conservation laws, but predicts results that hold for the full multidimensional system of model equations. The findings agree with experimental evidence and are appropriately embedded into the current state of knowledge of non-hyperbolic systems of conservation laws.

1. INTRODUCTION

Mathematical models for the sedimentation of polydisperse suspensions, consisting of small spherical particles belonging to a finite number of species that differ in size or density, are important to a variety of applications such as solid-liquid separation in mineral processing and wastewater treatment [60], classification [2, 73], fluidization [35, 36, 41], cast formation in the ceramic industry [9, 10], blood sedimentation in medicine [61], and volcanology [28]. For monodisperse suspensions of rigid spheres, widely used models for batch settling, continuous thickening and clarification go back to the kinematic sedimentation theory by KYNCH [20, 45], while a so-called phenomenological theory, as an extension of the kinematic model, is available for flocculated suspensions forming compressible sediments [15, 19]. The salient mathematical properties of, and differences between these models can best be studied in a spatially one-dimensional setup, such as a settling column, in which no equations for the motion of the mixture need to be solved. Then, the kinematic theory gives rise to a scalar first-order conservation law for the solids concentration involving a nonconvex

Date: June 6, 2001.

Key words and phrases. Polydisperse suspensions; hyperbolic conservation laws; hyperbolic-elliptic equations; mixed systems of conservation laws; kinematic model; instability region.

[a]Institute of Mathematics A, University of Stuttgart, Pfaffenwaldring 57, D-70569 Stuttgart, Germany,
e-mail: buerger@mathematik.uni-stuttgart.de, wendland@mathematik.uni-stuttgart.de,
WWW: http://www.mathematik.uni-stuttgart.de/mathA/lst6/buerger/buerger.en.html.

[b]Department of Mathematics, University of Bergen, Johs. Brunsgt. 12, N-5008 Bergen, Norway,
e-mail: kennethk@mi.uib.no, WWW: http://www.mi.uib.no/~kennethk/.

[c]Professor Emeritus, Department of Mathematics and Computer Science, Mount Allison University, Sackville, NB, E4l 1E8, Canada.
e-mail: sherpa@nbnet.nb.ca.

[*]Corresponding author.

flux density function, while the phenomenological theory produces a strongly degenerate parabolic-hyperbolic partial differential equation determining this quantity. At least in one space dimension, these monodisperse models are now well understood, have been subject of thorough existence and uniqueness analyses, can be simulated efficiently by numerical methods, and predict experimental results with reasonable accuracy, see [22] for a recent review.

Several attempts have been made to extend the monodisperse kinematic sedimentation theory to polydisperse suspensions, see [17] for an overview. All of them can (in one space dimension and for batch settling in a closed column) be written as a first-order system of N scalar conservation laws for N solid particle species,

$$\frac{\partial \phi_i}{\partial t} + \frac{\partial (\phi_i v_i)}{\partial z} = 0, \quad 0 \leq z \leq L, \quad t > 0, \quad i = 1, \ldots, N, \tag{1}$$

where t is time, z is height, ϕ_i is the local volumetric concentration of particle species i having diameter d_i and density ϱ_i, and v_i is the corresponding phase velocity. Here it is understood that $d_i \neq d_j$ or $\varrho_i \neq \varrho_j$ for $i \neq j$, $1 \leq i, j \leq N$. The models differ in the specific way that v_i is prescribed as a nonlinear function of the vector $\Phi := (\phi_1, \ldots, \phi_N)^{\mathrm{T}}$. In the sequel, we refer to each of these choices as 'models'. Thus (1) is a highly nonlinear, strongly coupled system of conservation laws, which under most circumstances can be solved only numerically. To get a first insight into the polydisperse sedimentation processes modeled by (1), this system was solved numerically for various values of N and models defining the velocities v_i [17, 18], where modern central difference schemes for hyperbolic systems of conservation laws were employed. Similar computations (based on numerical solution of the conservation equations) were performed by Flotats [32].

To proceed with the discussion, we recall here that the system of conservation laws

$$\frac{\partial \Phi}{\partial t} + \frac{\partial \mathbf{f}(\Phi)}{\partial z} = 0, \;\; 0 \leq z \leq L, \;\; t > 0; \quad \mathbf{f}(\Phi) = \big(f_1(\Phi), \ldots, f_N(\Phi)\big)^{\mathrm{T}} \tag{2}$$

is called *hyperbolic* if the Jacobian

$$\mathcal{J}_{\mathbf{f}}(\Phi) := \begin{bmatrix} \dfrac{\partial f_1(\Phi)}{\partial \phi_1} & \cdots & \dfrac{\partial f_1(\Phi)}{\partial \phi_N} \\ \vdots & \ddots & \vdots \\ \dfrac{\partial f_N(\Phi)}{\partial \phi_1} & \cdots & \dfrac{\partial f_N(\Phi)}{\partial \phi_N} \end{bmatrix} \tag{3}$$

has N real eigenvalues for all Φ, and *strictly hyperbolic* if these are in addition pairwise distinct.

The oscillation-free quality of all cited numerical simulations and their agreement with both physical insight and experimental evidence led to the tacit conjecture that the systems of conservation laws arising from polydisperse sedimentation models were always hyperbolic. As our analysis shows, this is not generally true, since certain models lead to Jacobians with at least one pair of complex conjugate eigenvalues on certain subregions of the set of admissible vectors Φ, while others do not for suspensions with the same size and density parameters.

It is the purpose of this contribution to demonstrate that mixed systems of conservation laws, rather than hyperbolic systems, provide the appropriate general mathematical framework for polydisperse sedimentation models. For the special case of bidisperse systems ($N = 2$), this means that hyperbolic-elliptic or mixed systems do occur. At the same time, we show that certain models lead (for $N = 2$ and particles of the same density) to systems that are indeed hyperbolic.

The importance of this observation lies in the fact that for bidisperse suspensions, the ellipticity condition coincides with the condition for the existence of instabilities in the polydisperse suspension, which in turn have been observed in experiments with particles of different densities [5, 71]. In this situation, the hyperbolic-elliptic type change behaviour is a *desirable* property for realistic bidisperse sedimentation models. Unfortunately, some bidisperse sedimentation models predict (due to their algebraic design) instability regions, that is, ellipticity regions for $N = 2$, under conditions in which they should *not* be expected, most notably for equal-density spheres, for which (with one exception that is discussed in Section 6.1) observations of unstable behaviour have never been reported.

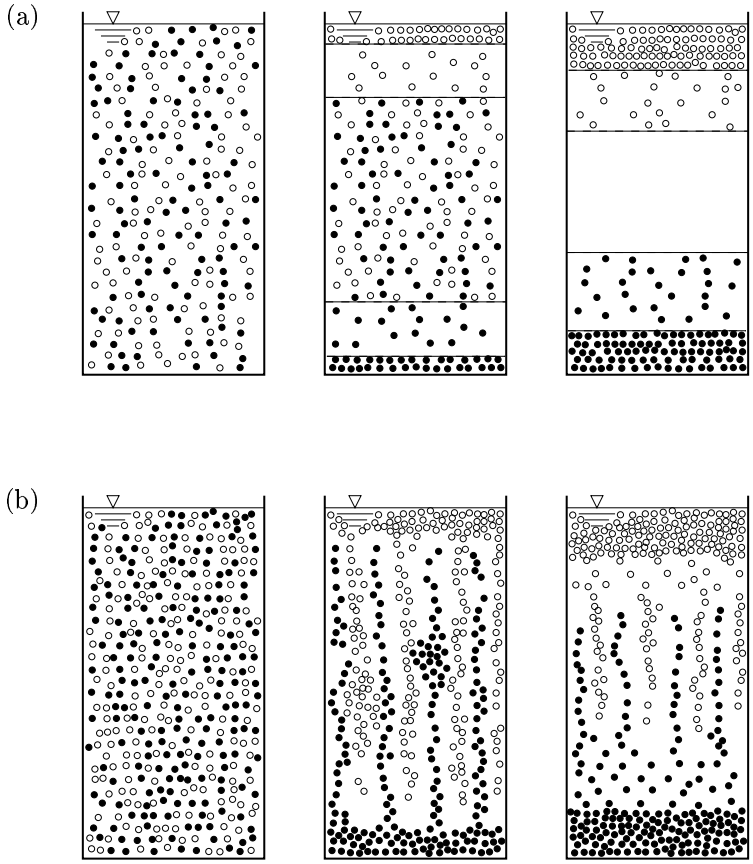

FIGURE 1. Sedimentation of a bidisperse suspension of heavy (•) and buoyant (creaming) (∘) particles: (a) stable demixing at small initial concentrations with upwards and downwards travelling horizontal concentration fronts, (b) unstable separation at large initial concentration with structure formation ("blobs" and vertical "columns"). The left drawings refer to the initial state and the middle and right diagrams to later stages of the separation.

To elaborate further the instability concept, consider a bidisperse suspension with one sedimenting phase, say Species 1, with $\varrho_1 > \varrho_f$, where ϱ_f is the density of the pure fluid, and a second buoyant or creaming Species 2 with $\varrho_2 < \varrho_f$. It is well known that the demixing behaviour of an initially homogeneous bidisperse suspension with particles having these properties strongly depends on the initial concentrations of each species. While small initial concentrations produce upwards and downwards traveling horizontal wave fronts (Figure 1(a)), such that the concentrations in the system at a given time essentially remain a function of height, larger concentrations lead to unstable behaviour that increases the rate of separation of the species [30, 71]. This instability leads to structures such as "blobs" or "columns" (Figure 1(b)) in which the lighter species moves upward and the heavier downward [5, 47, 71]. These structures are much longer lived than the transient currents (caused by inhomogeneities in local concentration) in monodisperse suspensions [5].

Based on a perturbation analysis of the three-dimensional model equations for the settling of a bidisperse suspension, BATCHELOR and JANSE VAN RENSBURG [5] derived the following condition for instability, which gives rise to the structures described above:

$$I_2 := \left(\frac{\partial \phi_1 v_1}{\partial \phi_1} - \frac{\partial \phi_2 v_2}{\partial \phi_2} \right)^2 + 4 \frac{\partial (\phi_1 v_1)}{\partial \phi_2} \frac{\partial (\phi_2 v_2)}{\partial \phi_1} < 0. \tag{4}$$

The instability criterion (4) was also validated experimentally by YAN and MASLIYAH [72] for the settling of heavy particles in an emulsion. In a very recent paper, BIESHEUVEL, VERWEIJ and BREEDVELD [11] evaluated condition (4) by replacing v_1 and v_2 (or, equivalently, $f_1 = \phi_1 v_1$ and $f_2 = \phi_2 v_2$) by the appropriate equations arising from the well-established MASLIYAH [51] and PATWARDHAN and TIEN [55] models, and determining instability regions in the (ϕ_1, ϕ_2)-plane in which (4) is satisfied if the ratios of the sizes and the reduced densities $\varrho_1 - \varrho_\mathrm{f}$ and $\varrho_2 - \varrho_\mathrm{f}$ are given. Although the authors of both papers [11] and [72] successfully determine instability regions which are consistent with experimental evidence, they do not interpret (4) as a condition for ellipticity of the model equations. In fact, the main idea of this contribution consists in showing that the loss of hyperbolicity can be regarded as an instability criterion for arbitrary N-disperse suspensions, although we shall discuss in this paper only the tridisperse case, for which a convenient instability criterion is available. It was the chief motivation of the present paper to extend the treatments in [5, 11, 72] to a general framework.

This paper is organized as follows. In Section 2, we first introduce the mass and linear momentum balance equations describing the polydisperse system as a mixture of $N + 1$ superimposed continua, the N solids species and the fluid. Then specific assumptions on the body force, the solid and fluid stress tensors, the pore pressure, the solid-fluid and the particle-particle interaction forces are stated. These assumptions are similar to those stated for monodisperse flocculated suspensions in [15, 19, 20]. However, we consider in this paper suspensions that form incompressible sediments not involving the concept of effective solid stress, and to make the final model not more complicated than is necessary to discuss the instability problem, assume that all viscosity effects are introduced by the viscous stress tensor of the fluid. On the other hand, the presence of several solids species requires a particle-particle interaction term. The decisive properties of the final model equations are given by the choice of the resistance coefficient for each particle species.

In Section 3, the linear momentum balance equations are first simplified as a consequence of a dimensional analysis, which justifies deleting all viscous and advective acceleration and the particle-particle interaction terms. Nevertheless, some viscosity is retained by not deleting the viscous term in the linear momentum balance of the fluid. The simplified linear momentum balances define a linear system of equations for the solid-fluid relative or slip velocities $\mathbf{u}_i := \mathbf{v}_i - \mathbf{v}_\mathrm{f}$, $i = 1, \ldots, N$, where $\mathbf{v}_i$ and $\mathbf{v}_\mathrm{f}$ are the three-dimensional phase velocities of particle species i and the fluid, respectively. This system can be solved explicitly. Neglecting the viscous terms in that system, we obtain $\mathbf{u}_1, \ldots, \mathbf{u}_N$ as explicit functions of the local concentration vector Φ if the resistance coefficient is specified. One common choice is related to the well-known RICHARDSON and ZAKI [59] hindered settling factor for monodisperse suspensions and was advanced in apparently independent papers by MASLIYAH [51] and LOCKETT and BASSOON [48]. We shall therefore refer to the resulting model, defined in terms of the explicit expressions of the slip velocities $\mathbf{u}_i$ or equivalently, the flux vector $\mathbf{f} = \mathbf{f}(\Phi)$, as the MASLIYAH-LOCKETT-BASSOON (MLB) model. The resulting three-dimensional model equations are then given by a system of conservation laws involving this flux density vector, plus a particular generalization of the Stokes system for incompressible flow for the mixture velocity field and the pore pressure. The derivation of multidimensional equations in Section 3 demonstrates that the instability criterion, although based on examination of a spatially one-dimensional system of conservation laws, indicates when instabilities in two- or three-dimensional model equations occur.

The MLB model can be viewed as a prototype of polydisperse sedimentation models in which information from the momentum balances of the solid species determines the slip velocities. A different family of models goes back to BATCHELOR [4], who postulated that in a dilute polydisperse suspension, the settling velocity of a sphere of species i, identified here with $\mathbf{v}_i$, is given by its Stokes velocity, multiplied by one plus a linear combination of the concentrations of all species. The coefficients in this linear combination have become famous as "Batchelor coefficients", and are calculated from first principles, see Section 3.5. Since the resulting formula can be used only in the dilute limit, several authors have proposed modifications to it that yield flux density vectors that are well-defined for the whole range of concentration values. We consider here both the modifications by DAVIS and GECOL [25, 26] and by HÖFLER and SCHWARZER [39, 40], to which we refer as the DG and HS models, respectively, but in contrast to the MLB model consider only

suspensions of spheres that differ in size but not in density. The DG and HS models ignore the linear momentum balances of the particles.

Section 4 is dedicated to the development of the new instability concept outlined in this introduction. In particular, we show that instability of a tridisperse suspension at a given concentration vector can be verified conveniently by evaluating a discriminant of the third-order characteristic polynomial of the Jacobian $\mathcal{J}_{\mathbf{f}}(\Phi)$, where $\mathbf{f}(\Phi)$ is defined by the different models. In practice, however, this has to be done numerically and one has to inspect each parameter choice separately, since the algebraic expressions involved become rather bulky. That this pointwise evaluation is a feasible way to evaluate the instability criterion is ensured by the fact that the (complex) eigenvalues of an $N \times N$ matrix are Hölder continuous functions of its coefficients with index $1/N$ (see [54]), and that the Jacobians in the present context are continuous functions of Φ.

In Section 5 we apply the instability criterion of Section 4 to the MLB, DG and HS models. We first prove that the MLB model is stable, i.e. hyperbolic, for bidisperse suspensions with particles that differ only in size, while it has been known from [11] that particles of different densities give rise (in general) to instability regions. We then determine numerically instability regions for a variety of mixed-density bi- and tridisperse suspensions. The numerical results suggest, however, that instability regions are of no practical importance for equal-sized spheres differing only slightly in density, since these are not located within the set of admissible concentration values.

We then show that the DG model with $N = 2$ is stable if the solid particles differ only moderately in size, say if the size ratio is not larger than about 5.5. Otherwise, the DG model starts to develop instability regions in the (ϕ_1, ϕ_2)-plane, which increase with the size ratio, and are located in regions of undoubtedly relevant concentration values. These instability regions are a consequence of the somewhat unphysical properties of the Batchelor coefficients. In addition, an example of a tridisperse instability region of the DG model is presented.

Finally, a very simple argument shows that the HS model is stable for any equal-density bidisperse suspension, if it is assumed that the Batchelor coefficients are nonpositive for these mixtures.

In Section 6 we briefly discuss two issues raised by our analysis that have not been considered so far. First, we briefly review some experimental studies of polydisperse sedimentation under the aspect of instability behaviour. Second, we discuss some of the non-standard properties and point out open problems of the non-hyperbolic, and in particular hyperbolic-elliptic, first-order systems of conservation laws to which polydisperse sedimentation models give rise.

2. Balance equations and constitutive assumptions for sedimentation of polydisperse suspensions

2.1. **Mass and linear momentum balance equations.** The local mass balance equations of the solid species and of the fluid can be written as

$$\frac{\partial \phi_i}{\partial t} + \nabla \cdot \big(\phi_i \mathbf{v}_i\big) = 0, \quad i = 1, \dots, N, \tag{5}$$

$$\frac{\partial \phi}{\partial t} - \nabla \cdot \big((1-\phi)\mathbf{v}_{\mathrm{f}}\big) = 0, \tag{6}$$

where $\phi := \phi_1 + \cdots + \phi_N$ denotes the total solids volume fraction. Defining the volume average velocity of the mixture $\mathbf{q} := (1-\phi)\mathbf{v}_{\mathrm{f}} + \phi_1 \mathbf{v}_1 + \cdots + \phi_N \mathbf{v}_N$, we derive easily that

$$\phi_i \mathbf{v}_i = \phi_i \big(\mathbf{u}_i + \mathbf{q} - (\phi_1 \mathbf{u}_1 + \cdots + \phi_N \mathbf{u}_N)\big), \quad i = 1, \dots, N, \tag{7}$$

hence the mass balance equations (5) can be rewritten in terms of $\mathbf{q}$ and $\mathbf{u}_1, \dots, \mathbf{u}_N$ as

$$\frac{\partial \phi_i}{\partial t} + \nabla \cdot \left(\phi_i \mathbf{u}_i + \phi_i \mathbf{q} - \phi_i \sum_{k=1}^{N} \phi_k \mathbf{u}_k\right) = 0, \quad i = 1, \dots, N. \tag{8}$$

The sum of all equations (5) and equation (6) produces the simple mass balance of the mixture

$$\nabla \cdot \mathbf{q} = 0. \tag{9}$$

The momentum balance equations read

$$\varrho_i\phi_i\frac{\mathrm{D}\mathbf{v}_i}{\mathrm{D}t} = \nabla\cdot\mathbf{T}_i + \varrho_i\phi_i\mathbf{b} + \mathbf{m}_i^{\mathrm{f}} + \sum_{k=1}^{N}\mathbf{m}_{ik}^{\mathrm{s}}, \quad i = 1,\ldots,N, \tag{10}$$

$$\varrho_{\mathrm{f}}(1-\phi)\frac{\mathrm{D}\mathbf{v}_{\mathrm{f}}}{\mathrm{D}t} = \nabla\cdot\mathbf{T}_{\mathrm{f}} + \varrho_{\mathrm{f}}(1-\phi)\mathbf{b} - \sum_{i=1}^{N}\mathbf{m}_i^{\mathrm{f}}. \tag{11}$$

Here $\mathbf{T}_i$ denotes the stress tensor of particle species i, $i = 1,\ldots,N$, $\mathbf{T}_{\mathrm{f}}$ that of the fluid, $\mathbf{b}$ is the body force, $\mathbf{m}_i^{\mathrm{f}}$ and $\mathbf{m}_{ij}^{\mathrm{s}}$ are the interaction forces per unit volume between solid species i and the fluid and between the solid species i and j, respectively, and we use the standard notation

$$\frac{\mathrm{D}\mathbf{v}}{\mathrm{D}t} := \frac{\partial\mathbf{v}}{\partial t} + (\mathbf{v}\cdot\nabla)\mathbf{v}.$$

2.2. **Body force.** In this work, it is assumed for simplicity that the only body force is gravity, $\mathbf{b} = -g\mathbf{k}$, where g is the acceleration of gravity and $\mathbf{k}$ is the upwards pointing unit vector. There is, however, no principal difficulty associated with including a centrifugal field, as e.g. in [16, 67].

2.3. **Solid and fluid stress tensors.** We assume that the stress tensors of the solid and fluid phases can be written as $\mathbf{T}_i = -p_i\mathbf{I} + \mathbf{T}_i^{\mathrm{E}}$ for $i = 1,\ldots,N$ and $\mathbf{T}_{\mathrm{f}} = -p_{\mathrm{f}}\mathbf{I} + \mathbf{T}_{\mathrm{f}}^{\mathrm{E}}$, respectively, where p_i denotes the phase pressure of particle species i, p_{f} that of the fluid, $\mathbf{I}$ denotes the identity tensor, and $\mathbf{T}_i^{\mathrm{E}}$ and $\mathbf{T}_{\mathrm{f}}^{\mathrm{E}}$ are the extra (or viscous) stress tensors of particle species i and the fluid, respectively. We could assume here that all viscous stress tensors $\mathbf{T}_i^{\mathrm{E}}$ and $\mathbf{T}_{\mathrm{f}}^{\mathrm{E}}$ are given by expressions that correspond, for example, to a viscous-linear fluid. This would require the definition of phase viscosities for each species and the fluid [19], which is still an open problem for monodisperse mixtures [66] and even more for polydisperse suspensions. However, we are mainly interested here in the continuity equations for the solid species, and assume that viscous effects due to the motion of the mixture are not dominant. Therefore we take the pragmatic approach [27] to assign all viscous effects to the fluid extra stress tensor. To make this simplification visible in the dimensional analysis, we assume that ν_0^{f} and $\nu_0^{\mathrm{s}} < \nu_0^{\mathrm{f}}$ are characteristic viscosities associated with the fluid and the solid species, respectively.

2.4. **Pore pressure.** The pressures p_i and p_{f} are theoretical variables that cannot be measured experimentally. For monodisperse compressible suspensions [19], these variables are expressed in terms of the pore pressure p and the effective solid stress σ_{e}. However, our particles are rigid incompressible spheres, so σ_{e} is assumed to be negligible, except in the packed bed.

We now relate the fluid phase pressure p_{f} and the solid species phase pressures to the pore pressure p. While the pore pressure p is defined within the fluid filling the interstices of the solids, the partial fluid pressure is defined in the fluid component occupying the whole volume of the mixture. Consider a cross-section S of a settling column and let $S_{\mathrm{f}} \subset S$ be the part of the cross section filled out by the fluid. We define the surface porosity $\epsilon := |S_{\mathrm{f}}|/|S|$, that is $dS_{\mathrm{f}} = \epsilon dS$. Then the surface forces exerted on the fluid in a cross section of the sediment are

$$\int_S p_{\mathrm{f}}\,dS = \int_{S_{\mathrm{f}}} p\,dS_{\mathrm{f}} = \int_S p(\epsilon dS). \tag{12}$$

Under fairly general conditions (see the Appendix), it is justified to assume that the surface porosity equals the volume porosity. Therefore, we may replace ϵ by $1-\phi$, and as a consequence of the localization theorem [37] we obtain from (12) $p_{\mathrm{f}} = (1-\phi)p$. The total stress of the mixture, p_{t}, can be written as $p_{\mathrm{t}} := p_{\mathrm{f}} + p_{\mathrm{s}} = (1-\phi)p + p_{\mathrm{s}}$, where the solids stress $p_{\mathrm{s}} := p_1 + \cdots + p_N$ is that part of the total stress which acts on the solid particles. If we assume that the cross-sectional area fraction of each species equals its volume fraction, we may conclude that $(\phi_i/\phi)p_{\mathrm{s}}$ is that part of the solids stress which acts on species i. It is therefore reasonable to relate the phase pressure p_i to the total pressure p_{t} by $p_i = \phi_i p_{\mathrm{t}}$ for $i = 1,\ldots,N$. Then $p_{\mathrm{t}} = p$, which could have been obtained from the corresponding equation for flocculated suspensions forming compressible sediments by setting $\sigma_{\mathrm{e}} = 0$.

2.5. **Solid-fluid interaction force.** In the case of a monodisperse suspension, the interaction force $\mathbf{m}$ between the fluid and the unique solid phase was modeled by the expression [19]

$$\mathbf{m} = \alpha(\phi)\mathbf{u} + \beta\nabla\phi + \gamma\frac{\mathrm{D}\mathbf{u}}{\mathrm{D}t}, \tag{13}$$

where α is the resistance coefficient, $\mathbf{u} := \mathbf{v}_\mathrm{s} - \mathbf{v}_\mathrm{f}$ is the solid-fluid relative velocity (or drift velocity), the coefficient β is shown to coincide with the pore pressure p, and the virtual mass term γ is neglected after the dimensional analysis. In the present case, the virtual mass terms will be neglected a priori, and we assume that the solid-fluid interaction term $\mathbf{m}_i^\mathrm{f}$ corresponding to species i is given by the following constitutive relationship, in which α_i denotes the resistance coefficient related to the transfer of momentum between the fluid and solid phase species i:

$$\mathbf{m}_i^\mathrm{f} = \alpha_i(\Phi)\mathbf{u}_i + \beta\nabla\phi_i, \quad i = 1, \ldots, N, \tag{14}$$

2.6. **Particle-particle interaction force.** In the specification of the interaction force between the different solid particle species, we follow SHIH et al. [62] and ARASTOOPOUR et al. [1] and consider the NAKAMURA and CAPES formula [53], which reads here

$$\mathbf{m}_{ij}^\mathrm{s} = \frac{3}{2}\varphi(1+e)\frac{\varrho_i\varrho_j\phi_i\phi_j(d_i+d_j)^2}{\varrho_i d_i^3 + \varrho_j d_j^3}\,\|\mathbf{v}_i - \mathbf{v}_j\|\,(\mathbf{v}_i - \mathbf{v}_j) \quad (i \neq j), \tag{15}$$

where the parameter φ accounts for non-head-on-collisions [62] and the restitution coefficient e equals zero for plastic and one for elastic collisions between particles. We anticipate that the term $\mathbf{m}_{ij}^\mathrm{s}$ will be eliminated due to the analysis, but note that the values of the combined parameter $\varphi(1+e)$ used by NAKAMURA and CAPES [53] varied between zero and 5, and that ARASTOOPOUR et al. [1] used the value $\varphi = 1$ and moreover found that numerical simulations of their multiphase flow model were not sensitive to the choice of φ.

The elimination of the particle-particle interaction term is not dependent on any particular formula. Though collisions seem likely in polydisperse suspensions, especially when some particles move upward, there is considerable experimental and theoretical evidence that $\mathbf{m}_{ij}^\mathrm{s}$ can be neglected at the very low Reynolds numbers considered here. VERHOEVEN [68] observed the fall of a single sphere through a dilute suspension of smaller, lighter spheres (cited in [64]). He noted that the larger sphere moved irregularly through the suspension, alternately gaining and losing companions: *"Though the spheres in these clusters were sometimes close together, they were always separated by fluid"*. Figure 7 of [69] shows the calculated trajectories of two sedimenting spheres on a collision course. Generally, they either "side-step" each other or rotate as a doublet and then separate. (Though permanent doublets are possible for two isolated spheres, interactions with other spheres would break them up in suspensions [64, 65].) Figure 6 of DAVIS [23] shows a similar doublet rotation in the calculated trajectories of a single sphere falling through a suspension of neutrally buoyant spheres. These "collisions" are damped by lubrication terms. As the gap between spheres narrows, the resistance to direct contact increases sharply [42]. Since particle-fluid interactions, including lubrication terms, are accounted for by $\mathbf{m}_i^\mathrm{f}$, direct contact between particles (which is important at large Reynolds numbers) plays a negligible role here.

2.7. **Solid-fluid interaction force at equilibrium.** Inserting the present constitutive assumptions into equations (10) and (11) leads to the following momentum balance equations for the solid phases and the fluid:

$$\varrho_i\phi_i\frac{\mathrm{D}\mathbf{v}_i}{\mathrm{D}t} = -\varrho_i\phi_i g\mathbf{k} + \nabla\cdot\mathbf{T}_i^\mathrm{E} - \phi_i\nabla p - p\nabla\phi_i + \alpha_i(\Phi)\mathbf{u}_i + \beta\nabla\phi_i + \sum_{k=1}^{N}\mathbf{m}_{ik}^\mathrm{s},\ i = 1, \ldots, N, \tag{16}$$

$$\varrho_\mathrm{f}(1-\phi)\frac{\mathrm{D}\mathbf{v}_\mathrm{f}}{\mathrm{D}t} = -\varrho_\mathrm{f}(1-\phi)g\mathbf{k} + \nabla\cdot\mathbf{T}_\mathrm{f}^\mathrm{E} - (1-\phi)\nabla p + p\nabla\phi - \beta\nabla\phi - \sum_{k=1}^{N}\alpha_k(\Phi)\mathbf{u}_k. \tag{17}$$

Note that in deriving (17) from (11), we have used $\nabla\phi = \nabla\phi_1 + \cdots + \nabla\phi_N$. To determine the parameter β, consider the polydisperse system at equilibrium ($t \to \infty$) in a settling column. At equilibrium, the solids and fluid phase velocities vanish, and the pore pressure reduces to the hydrostatic, i.e. $\mathbf{v}_\mathrm{f} = 0$, $\mathbf{u}_1 = \cdots = \mathbf{u}_N = 0$ and $\nabla p = -\varrho_\mathrm{f} g\mathbf{k}$ at equilibrium. Inserting

these assumptions into the fluid linear momentum balance equation (17), we obtain as in the monodisperse case $\beta = p$. Inserting this into (16) and (17) and rearranging (17), we obtain

$$\varrho_i \phi_i \frac{\mathrm{D}\mathbf{v}_i}{\mathrm{D}t} = -\varrho_i \phi_i g \mathbf{k} + \nabla \cdot \mathbf{T}_i^{\mathrm{E}} - \phi_i \nabla p + \alpha_i(\Phi)\mathbf{u}_i + \sum_{k=1}^{N} \mathbf{m}_{ik}^{\mathrm{s}}, \quad i = 1, \ldots, N, \tag{18}$$

$$\nabla p = -\varrho_{\mathrm{f}} g \mathbf{k} - \frac{1}{1-\phi} \sum_{k=1}^{N} \alpha_k(\Phi)\mathbf{u}_k - \varrho_{\mathrm{f}} \frac{\mathrm{D}\mathbf{v}_{\mathrm{f}}}{\mathrm{D}t} + \frac{1}{1-\phi} \nabla \cdot \mathbf{T}_{\mathrm{f}}^{\mathrm{E}}. \tag{19}$$

3. Dimensional analysis and final form of the model equations

3.1. **Dimensional analysis.** To further simplify the governing equations (8), (9), (18) and (19), we perform a dimensional analysis to detect which terms are negligible. To this end, we introduce dimensionless variables by referring all densities to the fluid density ϱ_{f}, all velocities to the velocity U, all lengths to a typical length L and all pressures to the hydrostatic pressure $\varrho_{\mathrm{f}} g L$. Here, we assume that U is the settling velocity of a single particle of the fastest settling species in an unbounded medium, and L is the depth of the settling vessel. A characteristic time is then given by $T = L/U$, which a single particle needs to travel from the top to the bottom of the vessel.

All dimensionless variables are marked by a star. A dimensionless gradient of a variable u is then defined by $\nabla^* u = L \nabla u$ and a dimensionless time derivative by $\partial u/\partial t^* = T \partial u/\partial t = (L/U)\partial u/\partial t$. Having in mind that the viscous stress tensors $\mathbf{T}_i^{\mathrm{E}}$ and $\mathbf{T}_{\mathrm{f}}^{\mathrm{E}}$ could be given by the expressions corresponding to a viscous-linear fluid, one can nondimensionalize these expressions by

$$\nabla^* \cdot \left(\mathbf{T}_i^{\mathrm{E}}\right)^* = \frac{L^2}{\varrho_{\mathrm{f}} \nu_0^{\mathrm{s}} U} \nabla \cdot \mathbf{T}_i^{\mathrm{E}}, \quad \nabla^* \cdot \left(\mathbf{T}_{\mathrm{f}}^{\mathrm{E}}\right)^* = \frac{L^2}{\varrho_{\mathrm{f}} \nu_0^{\mathrm{f}} U} \nabla \cdot \mathbf{T}_{\mathrm{f}}^{\mathrm{E}}, \tag{20}$$

where ν_0 denotes a typical kinematic viscosity, for example that of the pure fluid.

Using the Froude number of the flow Fr and the sedimentation Reynolds number Re defined by $\mathrm{Fr} := U^2/(gL)$ and $\mathrm{Re} := dU/\nu_0^{\mathrm{f}}$, where d is the size of the largest particles, we obtain the following dimensionless forms of equations (18) and (19):

$$\begin{aligned} \varrho_i^* \phi_i \mathrm{Fr} \frac{\mathrm{D}\mathbf{v}_i^*}{\mathrm{D}t^*} = {} & -\varrho_i^* \phi_i \mathbf{k} + \frac{d}{L} \frac{\nu_0^{\mathrm{s}}}{\nu_0^{\mathrm{f}}} \frac{\mathrm{Fr}}{\mathrm{Re}} \nabla^* \cdot \left(\mathbf{T}_i^{\mathrm{E}}\right)^* \\ & - \phi_i \nabla^* p^* + \alpha_i^*(\Phi)\mathbf{u}_i^* + \frac{L}{d} \mathrm{Fr} \sum_{k=1}^{N} \left(\mathbf{m}_{ik}^{\mathrm{s}}\right)^*, \quad i = 1, \ldots, N, \end{aligned} \tag{21}$$

$$\nabla^* p^* = -\mathbf{k} - \frac{1}{1-\phi} \sum_{k=1}^{N} \alpha_k^*(\Phi)\mathbf{u}_k^* - \mathrm{Fr} \frac{\mathrm{D}\mathbf{v}_{\mathrm{f}}^*}{\mathrm{D}t^*} + \frac{1}{1-\phi} \frac{d}{L} \frac{\mathrm{Fr}}{\mathrm{Re}} \nabla^* \cdot \left(\mathbf{T}_{\mathrm{f}}^{\mathrm{E}}\right)^*. \tag{22}$$

The following numerical values of the parameters are typical for the particulate systems considered here: $d = 10^{-4}\,\mathrm{m}$ (assumed size of a single sphere of the largest species), $g = 10\,\mathrm{m/s^2}$ (acceleration of gravity), $L = 1\,\mathrm{m}$ (typical height of a settling vessel), $U = 10^{-4}\,\mathrm{m/s}$ (settling velocity of a particle of the fastest species in an unbounded fluid), and $\nu_0^{\mathrm{f}} = 10^{-6}\,\mathrm{m^2/s}$ (kinematic viscosity of water). As mentioned above, it is reasonable to assume $\nu_0^{\mathrm{s}} < \nu_0^{\mathrm{f}}$, and due to our decision to move all effects of viscosity onto the fluid extra stress tensor we can assume $\nu_0^{\mathrm{s}}/\nu_0^{\mathrm{f}} \ll 1$. These values imply $\mathrm{Fr} = 10^{-9}$, $\mathrm{Re} = 10^{-2}$ and $d/L = 10^{-4}$. We assume that all dimensionless variables are of the order of magnitude $\mathcal{O}(1)$. Then we obtain, by discarding from the system of equations (21) all terms that have a coefficient which is 10^{-5} or smaller, and discarding the advective acceleration term from (22) but retaining the viscous term, the following simplified linear momentum balances from (21) and (22), which are written again here in their dimensional forms:

$$\alpha_i(\Phi)\mathbf{u}_i = \varrho_i \phi_i g \mathbf{k} + \phi_i \nabla p, \quad i = 1, \ldots, N, \tag{23}$$

$$\nabla p = -\varrho_{\mathrm{f}} g \mathbf{k} - \frac{1}{1-\phi} \sum_{k=1}^{N} \alpha_k(\Phi)\mathbf{u}_k + \frac{1}{1-\phi} \nabla \cdot \mathbf{T}_{\mathrm{f}}^{\mathrm{E}}. \tag{24}$$

Inserting (24) into (23), we obtain

$$\frac{\alpha_i(\Phi)(1-\phi)}{\phi_i}\mathbf{u}_i + \sum_{k=1}^{N}\alpha_k(\Phi)\mathbf{u}_k = \mathbf{r}_i, \quad \mathbf{r}_i := (1-\phi)\,(\varrho_i - \varrho_\mathrm{f})\,g\mathbf{k} + \nabla\cdot\mathbf{T}_\mathrm{f}^\mathrm{E}, \quad i = 1,\ldots,N. \tag{25}$$

3.2. **Explicit formula for the slip velocities $\mathbf{u}_i$.** Equations (25) form a linear system of N equations for the unknowns $\mathbf{u}_i$ that can be solved explicitly by the Sherman-Morrison formula, which states that for a matrix $\mathbf{A}$ of the type $\mathbf{A} = \mathbf{D} + \mathbf{x}\mathbf{y}^\mathrm{T}$, where $\mathbf{D}$ is an invertible diagonal matrix and $\mathbf{x}$ and $\mathbf{y}$ are given vectors, its inverse $\mathbf{A}^{-1}$ is given by

$$\mathbf{A}^{-1} = \left(\mathbf{D} + \mathbf{x}\mathbf{y}^\mathrm{T}\right)^{-1} = \mathbf{D}^{-1} - \left(1 + \mathbf{y}^\mathrm{T}\mathbf{D}^{-1}\mathbf{x}\right)^{-1}\mathbf{D}^{-1}\mathbf{x}\mathbf{y}^\mathrm{T}\mathbf{D}^{-1}. \tag{26}$$

Then the solution of the system (25) is

$$\mathbf{u}_i = \frac{\phi_i}{\alpha_i(\Phi)(1-\phi)}\left(\mathbf{r}_i - \sum_{k=1}^{N}\phi_k\mathbf{r}_k\right), \quad i = 1,\ldots,N. \tag{27}$$

Let $\varrho(\Phi) := (1-\phi)\varrho_\mathrm{f} + \phi_1\varrho_1 + \cdots + \phi_N\varrho_N$ denote the local density of the mixture and note that

$$\phi_1(\varrho_1 - \varrho_\mathrm{f}) + \cdots + \phi_N(\varrho_N - \varrho_\mathrm{f}) = \varrho(\Phi) - \varrho_\mathrm{f}. \tag{28}$$

Inserting the expressions $\mathbf{r}_1,\ldots,\mathbf{r}_N$ into (27) and neglecting the viscous term $\nabla\cdot\mathbf{T}_\mathrm{f}^\mathrm{E}$ leads to the following explicit equation for the slip velocities $\mathbf{u}_i$ as functions of Φ:

$$\mathbf{u}_i = \frac{\phi_i}{\alpha_i(\Phi)}\big(\varrho_i - \varrho(\Phi)\big)g\mathbf{k}, \quad i = 1,\ldots,N. \tag{29}$$

In order to ensure that $\mathbf{u}_i$ remains finite when $\phi_i \to 0$, we assume that

$$\alpha_i(\Phi) = \phi_i\xi_i(\Phi), \tag{30}$$

where the function ξ_i depends only on the diameter d_i, i.e. $\xi_i \equiv \xi_j$ if $d_i = d_j$, and remains bounded away from zero when $\phi_i \to 0$. Physically, this limit represents the velocity of a single particle of species i settling in a suspension of other species [64].

The derivation of (29) has closely followed Masliyah [51] who in turn used previous results from Wallis [70], but is here presented for three space dimensions. On the other hand, a slight generalization of an equation stated by Lockett and Bassoon [48] is

$$\mathbf{u}_i = \mathbf{u}_{\infty i}\frac{\varrho_i - \varrho(\Phi)}{\varrho_i - \varrho_\mathrm{f}}(1-\phi)^{n(\Phi)-2}, \quad i = 1,\ldots,N, \tag{31}$$

where

$$\mathbf{u}_{\infty i} = -\frac{d_i^2(\varrho_i - \varrho_\mathrm{f})g}{18\mu_\mathrm{f}}\mathbf{k}, \quad i = 1,\ldots,N \tag{32}$$

denotes the Stokes velocity of a single sphere of diameter d_i and density ϱ_i settling in pure fluid of density ϱ_f and dynamic viscosity μ_f. Equations (29) and (31) are equivalent if we choose

$$\frac{1}{\xi_i(\Phi)} = \frac{\phi_i}{\alpha_i(\Phi)} = -\frac{d_i^2}{18\mu_\mathrm{f}}(1-\phi)^{n(\Phi)-2}, \quad i = 1,\ldots,N. \tag{33}$$

This form, which is based on the Richardson-Zaki equation [59], has been fairly successful in interpreting experimental data [47]. The dependence of n on Φ is through wall effects, which are small when the diameter of the largest sphere is very small compared to the diameter of the settling vessel. In the sequel, we refer to Eq. (31) as the Masliyah-Lockett-Bassoon (MLB) model, whose value against alternate formulations was also emphasized recently by Biesheuvel [8].

Equation (33) can be written as

$$\xi_i(\Phi) = -\frac{18\mu_\mathrm{f}}{d_i^2 V(\Phi)}, \quad V(\Phi) := (1-\phi)^{n(\Phi)-2}. \tag{34}$$

To simplify the further discussion, we insert (30) and (34) into (29) to obtain the expression

$$\mathbf{u}_i = -\frac{\big(\varrho_i - \varrho(\Phi)\big)d_i^2 g}{18\mu_\mathrm{f}}V(\Phi)\mathbf{k}, \quad i = 1,\ldots,N, \tag{35}$$

where $V(\Phi)$ is an arbitrary suitable function (not necessarily that of the MLB model). In view of (28), it is convenient to introduce the reduced densities $\bar{\varrho}_\mathrm{s} := \varrho_\mathrm{s} - \varrho_\mathrm{f}$, $\bar{\varrho}_i := \varrho_i - \varrho_\mathrm{f}$, $i = 1, \ldots, N$, the vector $\bar{\boldsymbol{\varrho}} := (\bar{\varrho}_1, \ldots, \bar{\varrho}_N)^\mathrm{T}$, and the parameters

$$\mu = -\frac{g d_1^2}{18 \mu_\mathrm{f}}, \quad \delta_i = \frac{d_i^2}{d_1^2}, \quad i = 1, \ldots, N, \tag{36}$$

such that the final expression for the slip velocities reads

$$\mathbf{u}_i = \mu \delta_i (\bar{\varrho}_i - \bar{\boldsymbol{\varrho}} \cdot \Phi) V(\Phi) \mathbf{k}, \quad i = 1, \ldots, N. \tag{37}$$

3.3. **Final form of the model equations.** The final model equations are the continuity equations of the solids species (5) and of the mixture (9), the linear momentum balance of the fluid (24), and the equations (37) for the slip velocities $\mathbf{u}_i$, which have been obtained from the linear momentum balances of the solid species. Inserting (37) into (5) and (24), we obtain the final system of model equations:

$$\frac{\partial \phi_i}{\partial t} + \nabla \cdot \big(\phi_i \mathbf{q} + f_i(\Phi) \mathbf{k} \big) = 0, \quad i = 1, \ldots, N, \tag{38}$$

$$\nabla \cdot \mathbf{q} = 0, \tag{39}$$

$$\nabla p = -(\varrho_\mathrm{f} + \bar{\boldsymbol{\varrho}} \cdot \Phi) g \mathbf{k} + \frac{1}{1-\phi} \nabla \cdot \mathbf{T}_\mathrm{f}^\mathrm{E} \equiv -\varrho(\Phi) g \mathbf{k} + \frac{1}{1-\phi} \nabla \cdot \mathbf{T}_\mathrm{f}^\mathrm{E}. \tag{40}$$

Specifically for the MLB model, the components of the flux density vector $\mathbf{f}(\Phi)$ are given by

$$f_i(\Phi) = f_i^\mathrm{M}(\Phi) = \mu V(\Phi) \phi_i \left[\delta_i (\bar{\varrho}_i - \bar{\boldsymbol{\varrho}} \cdot \Phi) - \sum_{k=1}^{N} \delta_k \phi_k (\bar{\varrho}_k - \bar{\boldsymbol{\varrho}} \cdot \Phi) \right], \quad i = 1, \ldots, N. \tag{41}$$

Noting that $\mathbf{v}_\mathrm{f} = \mathbf{q} - (\phi_1 \mathbf{u}_1 + \cdots + \phi_N \mathbf{u}_N)$, we can rewrite $\mathbf{T}_\mathrm{f}^\mathrm{E}$ in terms of the sought mixture velocity $\mathbf{q}$ and the slip velocities $\mathbf{u}_i$, which are now given functions of Φ. For example, if we set

$$\mathbf{T}_\mathrm{f}^\mathrm{E} = \mu(\phi) \left[\nabla \mathbf{v}_\mathrm{f} + (\nabla \mathbf{v}_\mathrm{f})^\mathrm{T} - \frac{2}{3} (\nabla \cdot \mathbf{v}_\mathrm{f}) \mathbf{I} \right] \tag{42}$$

as for a standard viscous-linear fluid, we obtain the linear momentum balance

$$\nabla p = -\varrho(\Phi) g \mathbf{k} + \frac{1}{1-\phi} \left\{ \Big[\big(\nabla \mu(\phi) \big)^\mathrm{T} \big(\nabla \mathbf{q} + (\nabla \mathbf{q})^\mathrm{T} \big) + \mu(\phi) \Delta \mathbf{q} \Big] + \nabla \cdot \big(\mu(\phi) \mathbf{U}(\Phi, \nabla \Phi) \big) \right\}, \tag{43}$$

where μ is a concentration-dependent viscosity function and

$$\mathbf{U}(\Phi, \nabla \Phi) := \sum_{i=1}^{N} \nabla(\phi_i \mathbf{u}_i) + \big(\nabla(\phi_i \mathbf{u}_i) \big)^\mathrm{T} - \frac{2}{3} \big(\nabla \cdot (\phi_i \mathbf{u}_i) \big) \mathbf{I}. \tag{44}$$

Eq. (43) can of course be written as

$$\nabla p = -\varrho(\Phi) g \mathbf{k} + \frac{1}{1-\phi} \Big[\big(\nabla \mu(\phi) \big)^\mathrm{T} \big(\nabla \mathbf{q} + (\nabla \mathbf{q})^\mathrm{T} \big) + \mu(\phi) \Delta \mathbf{q} \Big] + \mathbf{g}(\Phi, \nabla \Phi, \nabla^2 \Phi), \tag{45}$$

where $\mathbf{g}$ is a function depending on Φ and the derivatives of its components of up to second order.

Observe that in the absence of solid particles, i.e. when $\Phi \equiv 0$, Equations (39) and (40) form the Stokes system for an incompressible fluid for the velocity $\mathbf{q}$ (then identical to the fluid phase velocity $\mathbf{v}_\mathrm{f}$) and the pressure p.

3.4. **Initial and boundary conditions in one space dimension.** In one space dimension, Eq. (39) turns into $\partial q / \partial z = 0$, that is $q = q(t)$. In a closed vessel, the mixture velocity at the bottom vanishes, hence $q \equiv 0$ and the remaining equations that actually have to be solved are the system of conservation laws (2), together with an initial concentration distribution

$$\Phi(z, 0) = \Phi^0(z) \in \mathcal{D}_{\phi_\mathrm{max}}, \quad 0 \le z \le L, \tag{46}$$

where $\mathcal{D}_{\phi_\mathrm{max}}$ is the set of admissible concentration values defined by

$$\mathcal{D}_{\phi_\mathrm{max}} := \big\{ \Phi = (\phi_1, \ldots, \phi_N) \in \mathbb{R}^N : \phi_1 \ge 0, \ldots, \phi_N \ge 0; \ \phi_1 + \cdots + \phi_N \le \phi_\mathrm{max} \big\},$$

and $0 < \phi_{\max} \leq 1$ in turn denotes the maximum admissible cumulative solids concentration, and the zero flux boundary conditions

$$\mathbf{f}|_{z=0} = 0, \quad \mathbf{f}|_{z=L} = 0, \quad t > 0. \tag{47}$$

In this paper, we do not present exact or numerical solutions of the initial-boundary value problem (2), (46), (47), but refer to our previous papers [17, 18] for a collection of examples.

3.5. BATCHELOR's **formula and its modifications.** The previous analysis has been based on both the mass and linear momentum balance equations for each particle species. A different approach is due to BATCHELOR [4], who postulated that in a dilute suspension, the phase velocity of spheres of species i having diameter d_i can be approximated by the expression

$$\mathbf{v}_i = \mathbf{v}_i(\Phi) = \mathbf{u}_{\infty i}\left(1 + \mathbf{e}_i^{\mathrm{T}}\mathbf{S}\Phi\right), \tag{48}$$

where $\mathbf{e}_i$ is the N-dimensional vector having the entries one at the i-th position and zero otherwise, $\mathbf{S} = (S_{ij})_{1\leq i,j\leq N}$ is the $N \times N$ matrix of the so-called Batchelor coefficients, and $\mathbf{u}_{\infty i}$ is the Stokes velocity of particle species i given by Eq. (32).

The entries S_{ij} of the matrix $\mathbf{S}$ depend on the diameter and reduced density ratios $\lambda_{ij} := d_j/d_i$ and $\bar{\varrho}_j/\bar{\varrho}_i$ of particle species i and j. Numerical values of these coefficients are given for several special cases by BATCHELOR and WEN [6], which represent numerical evaluations of integrals derived in [4], i.e., the coefficients S_{ij} are deduced from first principles.

In this paper, we limit the discussion to those cases where all particles are of the same density, $\bar{\varrho}_j/\bar{\varrho}_i = 1$, and the coefficients S_{ij} are given by

$$S_{ij} = \beta_0 + \beta_1\lambda_{ij} + \beta_2\lambda_{ij}^2 + \beta_3\lambda_{ij}^3; \quad \beta_k \leq 0,\ k = 0,\ldots,3. \tag{49}$$

Cases included here are the parameter vectors $\boldsymbol{\beta} = (\beta_0,\ldots,\beta_3)$ with

$$\boldsymbol{\beta} = (-3.50, -1.10, -1.02, -0.002) \tag{50}$$

$$\text{and} \quad \boldsymbol{\beta} = (-3.42, -1.96, -1.21, -0.013) \tag{51}$$

determined by DAVIS and GECOL [25] by fitting numerical data of BATCHELOR and WEN [6] to cubic polynomials, where $0 \leq \lambda_{ij} \leq 8$ and formula (50) applies to large and (51) to small particle Péclet numbers, and the values $\boldsymbol{\beta} = (-3.52, -1.04, -1.03, 0)$ utilized by HÖFLER and SCHWARZER [40], see also [18].

The formulas (48) are valid only in the dilute limit $\Phi \to 0$, and both DAVIS and GECOL [25] and HÖFLER and SCHWARZER [40] suggested modifications to (48) in order to obtain well-defined model equations for all $\Phi \in \mathcal{D}_{\phi_{\max}}$.

In order to make $\mathbf{v}_i = 0$ when $\phi = \phi_{\max}$ and to retain the same settling velocities as those given by (48) in the dilute limit $\Phi \to 0$, DAVIS and GECOL [25] propose utilizing a flux vector $\mathbf{f}^{\mathrm{DG}}(\Phi)$ having the following components, which are calculated from the Batchelor coefficients S_{ij}:

$$f_i^{\mathrm{DG}}(\Phi) = \mu\bar{\varrho}_{\mathrm{s}}\delta_i\phi_i\left(1 + \sum_{j=1}^{N}\left(S_{ij} - S_{ii}\right)\phi_j\right)(1-\phi)^{-S_{ii}}, \quad i = 1,\ldots,N. \tag{52}$$

As stated in [25], the salient features of the expression (52) are that it agrees with BATCHELOR's equations (48) in the dilute limit $\phi \ll 1$, that it merely requires BATCHELOR's sedimentation coefficients as parameters, and that for the monodisperse case $N = 1$ it reduces to the RICHARDSON-ZAKI [59] equation $f(\phi) = \mu\bar{\varrho}_{\mathrm{s}}\phi(1-\phi)^n$ with the exponent n replaced by $-S_{ii}$.

In a similar attempt to make $\mathbf{v}_i = 0$ when $\phi = \phi_{\max}$, HÖFLER and SCHWARZER [39, 40] replace Eq. (48) by the expression

$$\mathbf{v}_i = \mathbf{u}_{\infty i}\exp\left(\mathbf{e}_i^{\mathrm{T}}\mathbf{S}\Phi + n\bar{\phi}\right)\left(1 - \bar{\phi}\right)^n, \tag{53}$$

where $\bar{\phi} := \phi/\phi_{\max}$, and the exponent $n = 2$ is considered [40]. The velocities $\mathbf{v}_i$ given by (53) vanish for $\phi = \phi_{\max}$ and have the same partial derivatives for $\Phi = 0$ as (48). Using the parameters μ and $\delta_1,\ldots,\delta_N$ defined in (36), we obtain

$$f_i(\Phi) = f_i^{\mathrm{HS}}(\Phi) = \mu\bar{\varrho}_{\mathrm{s}}\delta_i\phi_i\exp\left(\mathbf{e}_i^{\mathrm{T}}\mathbf{S}\Phi + n\bar{\phi}\right)\left(1 - \bar{\phi}\right)^n. \tag{54}$$

In the sequel, we refer to Eqns. (52) and (54) as the DG and HS models, respectively.

3.6. **The special case $N = 2$.** We shall write out the system (2) for the two simplest non-trivial cases: the settling of initially homogeneous suspensions with two different particle sizes which are of the same density and with one particle size but different densities, respectively. The MLB model, as expressed by (31), handles both cases, in which we obtain

$$\mathbf{f}^{\mathrm{M}}(\Phi) = \mu\bar{\varrho}_{\mathrm{s}}V(\Phi)(1-\phi_1-\phi_2)\begin{pmatrix} \phi_1(1-\phi_1)-\delta_2\phi_1\phi_2 \\ \delta_2\phi_2(1-\phi_2)-\phi_1\phi_2 \end{pmatrix}, \tag{55}$$

$$\mathbf{f}^{\mathrm{M}}(\Phi) = \mu V(\Phi)\begin{pmatrix} \phi_1\big[(1-\phi_1)\big((1-\phi_1)\bar{\varrho}_1-\phi_2\bar{\varrho}_2\big)-\phi_2\big(-\phi_1\bar{\varrho}_1+(1-\phi_2)\bar{\varrho}_2\big)\big] \\ \phi_2\big[-\phi_1\big((1-\phi_1)\bar{\varrho}_1-\phi_2\bar{\varrho}_2\big)+(1-\phi_2)\big(-\phi_1\bar{\varrho}_1+(1-\phi_2)\bar{\varrho}_2\big)\big] \end{pmatrix}, \tag{56}$$

repectively. The DG and HS flux density vectors for equal-density particles read

$$\mathbf{f}^{\mathrm{DG}}(\Phi) = \mu\bar{\varrho}_{\mathrm{s}}\begin{pmatrix} \phi_1\big(1+(S_{12}-S_{11})\phi_2\big)(1-\phi_1-\phi_2)^{-S_{11}} \\ \delta_2\phi_2\big(1+(S_{21}-S_{22})\phi_1\big)(1-\phi_1-\phi_2)^{-S_{22}} \end{pmatrix}, \tag{57}$$

$$\mathbf{f}^{\mathrm{HS}}(\Phi) = \mu\bar{\varrho}_{\mathrm{s}}\left(1-\frac{\phi_1+\phi_2}{\phi_{\max}}\right)^n\begin{pmatrix} \phi_1\exp\big((S_{11}\phi_1+S_{12}\phi_2)+(n/\phi_{\max})(\phi_1+\phi_2)\big) \\ \delta_2\phi_2\exp\big((S_{21}\phi_1+S_{22}\phi_2)+(n/\phi_{\max})(\phi_1+\phi_2)\big) \end{pmatrix}. \tag{58}$$

4. The instability criterion

In the case $N = 2$, the characteristic polynomial of the Jacobian $\mathcal{J}_{\mathbf{f}}(\phi_1,\phi_2)$ reads

$$p_2(\lambda;\Phi) = \det\big(\mathcal{J}_{\mathbf{f}}(\Phi)-\lambda\mathbf{I}\big) = \left(\lambda-\frac{1}{2}\left[\frac{\partial f_1(\phi_1,\phi_2)}{\partial\phi_1}+\frac{\partial f_2(\phi_1,\phi_2)}{\partial\phi_2}\right]\right)^2-\frac{1}{4}I_2. \tag{59}$$

We have $p_2(\lambda;\phi_1,\phi_2) > 0$ for all λ and thus has one pair of complex conjugate roots such that the system (2) is elliptic, if and only if the instability condition (4), which in our terms reads

$$I_2 \equiv \left(\frac{\partial f_1(\phi_1,\phi_2)}{\partial\phi_1}-\frac{\partial f_2(\phi_1,\phi_2)}{\partial\phi_2}\right)^2+4\frac{\partial f_1(\phi_1,\phi_2)}{\partial\phi_2}\frac{\partial f_2(\phi_1,\phi_2)}{\partial\phi_1} < 0, \tag{60}$$

is satisfied. Thus in the case $N = 2$ the instability region, that is the subset of $\mathcal{D}_{\phi_{\max}}$ where the criterion (4) from [5] is satisfied, coincides with the region where the 2×2 system of conservation laws (2) changed from first-order hyperbolic to first-order elliptic type.

We observe that the instability criterion, predicting the existence of perturbations, is related to the loss of hyperbolicity of the model equations in a subregion of $\mathcal{D}_{\phi_{\max}}$. In fact, with "ellipticity" replaced by "loss of hyperbolicity", this criterion becomes independent of the number of species, since only in the case $N = 2$ are the equations either hyperbolic or elliptic. To show that loss of hyperbolicity can indeed be viewed as a general instability criterion for any polydisperse suspension, we closely follow the analysis by Batchelor and Janse van Rensburg [5], but extend their treatment from bidisperse to N-disperse suspensions.

The linearized form of (38) for a small disturbance to the homogeneous suspension is then

$$\frac{\partial\phi_i}{\partial t}+\sum_{j=1}^{N}\left(\frac{\partial f_i(\Phi)}{\partial\phi_j}\mathbf{k}\right)^{(0)}\cdot\nabla\phi_j = 0, \quad i = 1,\dots,N. \tag{61}$$

We then investigate, as in [5], the evolution of a disturbed state of the form

$$\phi_i = \phi_i^{(0)}+A_i\exp\big(\sigma t+\mathrm{i}\mathbf{h}\cdot(\mathbf{x}-\mathbf{c}t)\big), \quad i = 1,\dots,N. \tag{62}$$

Here σ, $\mathbf{h}$ and $\mathbf{c}$ are real, due to the assumption that a perturbation of arbitrary initial form can be expressed as a sum or integral of such three-dimensional Fourier components evolving independently. Inserting (62) into (61), we obtain

$$(\sigma-\mathrm{i}\mathbf{h}\cdot\mathbf{c})A_i+\mathrm{i}\sum_{j=1}^{N}\mathbf{h}\cdot\left(\frac{\partial f_i(\Phi)}{\partial\phi_j}\mathbf{k}\right)^{(0)}A_j = 0. \tag{63}$$

We now let

$$k_{ij} = \mathbf{h}\cdot\left(\frac{\partial f_i(\Phi)}{\partial\phi_j}\mathbf{k}\right)^{(0)}, \quad 1\le i,j\le N. \tag{64}$$

Eliminating the amplitudes A_i, $i = 1, \ldots, N$, we find that the matrix $(\sigma - \mathrm{i}\mathbf{h}\cdot\mathbf{c})\mathbf{I} + \mathrm{i}\mathbf{K}$ must be singular, where $\mathbf{I}$ denotes the $N \times N$ unity matrix and $\mathbf{K} = (k_{ij})_{i,j=1,\ldots,N}$. Then the following equation must be valid (otherwise all amplitudes vanish):

$$\det\big((\sigma - \mathrm{i}\mathbf{h}\cdot\mathbf{c})\mathbf{I} + \mathrm{i}\mathbf{K}\big) = 0. \tag{65}$$

Condition (65) is obviously equivalent to

$$\det\big(\mathbf{K} - (\sigma\mathrm{i} + \mathbf{h}\cdot\mathbf{c})\mathbf{I}\big) = 0, \tag{66}$$

hence $\sigma\mathrm{i} + \mathbf{h}\cdot\mathbf{c}$ must be an eigenvalue λ of the matrix $\mathbf{K}$. Consequently, a necessary and sufficient condition for an exponentially growing disturbance to exist, that is that (66) has a positive solution σ, is that the matrix $\mathbf{K}$ possesses an eigenvalue λ with positive imaginary part. However, since $\mathbf{K}$ is real, this means that there should exist at least one pair of complex conjugate eigenvalues (one of which of course has positive imaginary part). Obviously, we may write

$$k_{ij} = h\cos\theta\left(\frac{\partial f_i(\Phi)}{\partial\phi_j}\right)^{(0)}, \tag{67}$$

where θ is the angle made with the upward vertical by the wavenumber vector $\mathbf{h}$. Since $\mathbf{c}$ must also be a vertical vector, we can furthermore write $\mathbf{h}\cdot\mathbf{c} = hc\cos\theta$. We then have $\mathbf{K} = h\cos\theta\mathcal{J}_\mathbf{f}(\Phi^{(0)})$ and see that the instability criterion is equivalent to the existence of a pair of complex conjugate eigenvalues λ, $\bar{\lambda}$ of the Jacobian $\mathcal{J}_\mathbf{f}(\Phi^{(0)})$. In other words, there must be a state $\Phi = \Phi^{(0)}$ at which the system of conservation laws

$$\frac{\partial\phi_i}{\partial t} + \nabla\cdot\big(f_i(\Phi)\mathbf{k}\big) \equiv \frac{\partial\phi_i}{\partial t} + \frac{\partial f_i(\Phi)}{\partial z} = 0, \quad i = 1, \ldots, N \tag{68}$$

fails to be hyperbolic. In the case $N = 2$, this means, of course, that the system must be elliptic.

Unfortunately, polydisperse sedimentation models do not give rise to Jacobians for which it is easy to decide (as, for example, for symmetric matrices) whether they possess only real or both real and complex conjugate eigenvalues. However, for tridisperse suspensions it is possible to decide on hyperbolicity, and thus to determine whether the equations are stable, by evaluating one scalar discriminant function defined in a similar way as I_2, whose sign determines the instability region. Namely, for $N = 3$ the characteristic polynomial of the Jacobian $\mathcal{J}_\mathbf{f}(\Phi)$ takes the form

$$p_3(\lambda;\Phi) = \lambda^3 + r(\Phi)\lambda^2 + s(\Phi)\lambda + t(\Phi), \tag{69}$$

where the leading coefficient has been normalized to one and the functions r, s and t are given by

$$r = r(\Phi) = -\mathrm{tr}\,\mathcal{J}_\mathbf{f}(\Phi) = -\left(\frac{\partial f_1}{\partial\phi_1} + \frac{\partial f_2}{\partial\phi_2} + \frac{\partial f_3}{\partial\phi_3}\right), \quad t = t(\Phi) = -\det\mathcal{J}_\mathbf{f}(\Phi),$$

$$s = s(\Phi) = -\left(\frac{\partial f_1}{\partial\phi_3}\frac{\partial f_3}{\partial\phi_1} + \frac{\partial f_1}{\partial\phi_2}\frac{\partial f_2}{\partial\phi_1} + \frac{\partial f_2}{\partial\phi_3}\frac{\partial f_3}{\partial\phi_2} - \frac{\partial f_1}{\partial\phi_1}\frac{\partial f_2}{\partial\phi_2} - \frac{\partial f_1}{\partial\phi_1}\frac{\partial f_3}{\partial\phi_3} - \frac{\partial f_2}{\partial\phi_2}\frac{\partial f_3}{\partial\phi_3}\right).$$

It is well known [14] that the equation $p_3(\lambda;\Phi) = 0$ has one real and one pair of complex conjugate solutions if and only if with

$$p = p(\Phi) := s - \frac{1}{3}r^2, \quad q = q(\Phi) := \frac{2}{27}r^3 - \frac{1}{3}rs + t,$$

the following inequality holds:

$$I_3(\Phi) := \left(\frac{p}{3}\right)^3 + \left(\frac{q}{2}\right)^2 = \frac{1}{27}s^3 - \frac{1}{108}s^2r^2 + \frac{1}{4}t^2 + \frac{1}{27}r^3t - \frac{1}{6}rst > 0. \tag{70}$$

In most circumstances, it will be very cumbersome to calculate I_3 for a given model by hand when a general result with respect to the size and density parameters is sought. However, the criterion (70) is useful when the stability of a model for given sizes and densities is to be examined, such that it is sufficient to compute I_3 numerically for a dense set of test vectors $\Phi \in \mathcal{D}_{\phi_{\max}}$. Section 5 includes some numerical calculations of instability regions for $N = 3$.

Note that wherever one of three particle species in a tridisperse suspension is absent, say Species 3, the suspension behaves as a bidisperse suspension of Species 1 and 2. In this case, $\phi_3 = 0$, such that $f_3(\cdot,\cdot,0) \equiv 0$ and thus $t(\cdot,\cdot,0) \equiv 0$. Then the bidisperse suspension is stable if

$$I_3 = -\frac{1}{108}s^2(r^2 - 4s) > 0,$$

that is if $r^2 - 4s < 0$. Since $I_2 \equiv r^2 - 4s$ for a bidisperse suspension of Species 1 and 2, we see that (70) is a more general criterion than, and in particular includes (60). Thus the intersections of the three-dimensional instability regions determined by (70) with the planes $\phi_i = 0$, $i = 1,2,3$ coincide with the corresponding bidisperse instability regions.

A related observation is that whenever $N_0 < N$ of the species in an N-disperse suspension have size or density ratios that produce an N_0-dimensional instability region with the bidisperse equations, we know that there also exists an instability region in the N-dimensional domain. Moreover, by the continuity of the eigenvalues with respect to $\phi_1, \ldots, \phi_N$, this instability region will be of nonzero N-dimensional volume.

Finally, we remark that it would be possible to extend the explicit instability criterion based on evaluating a discriminant of the characteristic polynomial also to the case $N = 4$. We will not pursue this further here.

5. Instability regions of selected polydisperse sedimentation models

5.1. **Stability of the Masliyah-Lockett-Bassoon model equations.** We limit ourselves here to a constant Richardson-Zaki exponent $n = n(\Phi)$ [59], such that $V(\Phi) = V(\phi) = (1-\phi)^{n-2}$. Then, differentiating (41) with respect to ϕ_k, we obtain

$$\begin{aligned}\frac{\partial f_i^{\mathrm{M}}(\Phi)}{\partial \phi_k} = \mu(1-\phi)^{n-3}\Bigg\{&\big((1-\phi)\delta_{ik} - (n-2)\phi_i\big)\left[\delta_i(\bar{\varrho}_i - \bar{\boldsymbol{\varrho}}\cdot\Phi) - \sum_{j=1}^{N}\delta_j\phi_j(\bar{\varrho}_j - \bar{\boldsymbol{\varrho}}\cdot\Phi)\right]\\ &+ (1-\phi)\phi_i\left[-\delta_i\bar{\varrho}_k - \delta_k(\bar{\varrho}_k - \bar{\boldsymbol{\varrho}}\cdot\Phi) + \bar{\varrho}_k\sum_{j=1}^{N}\delta_j\phi_j\right]\Bigg\},\end{aligned} \tag{71}$$

where $\delta_{ik} = 1$ if $i = k$ and $\delta_{ik} = 0$ otherwise. For the special cases of spheres of equal density, but different sizes, and that of equal size but different densities, we obtain the respective derivatives

$$\frac{\partial f_i^{\mathrm{M}}}{\partial \phi_k} = \mu\bar{\varrho}_{\mathrm{s}}(1-\phi)^{n-2}\Big\{(1-\phi)\delta_{ik} + \phi_i\big(-(n-1)\big[\delta_i - \delta_1\phi_1 - \cdots - \delta_N\phi_N\big] + (1-\phi)\delta_k\big)\Big\}, \tag{72}$$

$$\begin{aligned}\frac{\partial f_i^{\mathrm{M}}}{\partial \phi_k} = \mu(1-\phi)^{n-2}\Big\{&(1-\phi)\delta_{ik} + \phi_i\Big(-(n-2)\big[\bar{\varrho}_i + (\phi-2)\bar{\boldsymbol{\varrho}}\cdot\Phi\big]\\ &- (1-\phi)\big[(2-\phi)\bar{\varrho}_k - \bar{\boldsymbol{\varrho}}\cdot\Phi\big]\Big)\Big\}.\end{aligned} \tag{73}$$

We first apply the instability criterion (60) to either system (72) or (73). Biesheuvel et al. [11] recently presented a thorough numerical evaluation of the instability criterion (60) for the MLB model and $N = 2$ with bidisperse suspensions of species differing only in size, only in density, and both. Some of their results are presented as instability diagrams, that is as contours of the instability region in the (ϕ_1, ϕ_2)-plane. We adopt this representation here and discuss a few bidisperse cases where additional insight can be provided. Consider now a bidisperse suspension with particles of different sizes and the same density (with the flux vector $\mathbf{f}^{\mathrm{M}}$ given by (55)). Then

$$\begin{aligned}\frac{\partial f_1^{\mathrm{M}}}{\partial \phi_1} &= \mu\bar{\varrho}_{\mathrm{s}}(1-\phi)^{n-2}\Big[(1-\phi)(1-\phi_1-\delta_2\phi_2) + \phi_1\big(-(n-1)(1-\phi_1-\delta_2\phi_2) - (1-\phi)\big)\Big],\\ \frac{\partial f_1^{\mathrm{M}}}{\partial \phi_2} &= \mu\bar{\varrho}_{\mathrm{s}}(1-\phi)^{n-2}\phi_1\big(-(n-1)(1-\phi_1-\delta_2\phi_2) - \delta_2(1-\phi)\big),\\ \frac{\partial f_2^{\mathrm{M}}}{\partial \phi_1} &= \mu\bar{\varrho}_{\mathrm{s}}(1-\phi)^{n-2}\phi_2\big(-(n-1)(\delta_2-\phi_1-\delta_2\phi_2) - (1-\phi)\big),\end{aligned}$$

$$\frac{\partial f_2^{\mathrm{M}}}{\partial \phi_2} = \mu \bar{\varrho}_{\mathrm{s}} (1-\phi)^{n-2} \Big[(1-\phi)(\delta_2 - \phi_1 - \delta_2\phi_2) + \phi_2 \big(-(n-1)(\delta_2 - \phi_1 - \delta_2\phi_2) - \delta_2(1-\phi) \big) \Big].$$

We now prove that the MLB equations are in fact stable for $N = 2$, all values of $\delta_2 > 0$, and for all $\phi_1, \phi_2 \in \mathcal{D}_1$ by evaluating explicitly the instability criterion (60). To this end, we first define

$$\begin{aligned}
\tilde{I}_2 :=& \big(\mu \bar{\varrho}_2 (1-\phi)^{n-2}\big)^{-2} I_2 \\
=& \Big[(1-\phi)(1-\delta_2) + \phi_1 \big(-(n-1)(1-\phi_1-\delta_2\phi_2) - (1-\phi) \big) \\
&\qquad - \phi_2 \big(-(n-1)(\delta_2 - \phi_1 - \delta_2\phi_2) - \delta_2(1-\phi) \big) \Big]^2 \\
&+ 4\phi_1\phi_2 \big(-(n-1)(1-\phi_1-\delta_2\phi_2) - \delta_2(1-\phi) \big) \big(-(n-1)(\delta_2 - \phi_1 - \delta_2\phi_2) - (1-\phi) \big) \\
=& (1-\phi)^2(1-\delta_2)^2 + \phi_1^2 \big(-(n-1)(1-\phi_1-\delta_2\phi_2) - (1-\phi) \big)^2 \\
&+ \phi_2^2 \big(-(n-1)(\delta_2 - \phi_1 - \delta_2\phi_2) - \delta_2(1-\phi) \big)^2 \\
&+ 2\phi_1(1-\delta_2)(1-\phi) \big(-(n-1)(1-\phi_1-\delta_2\phi_2) - (1-\phi) \big) \\
&- 2\phi_2(1-\delta_2)(1-\phi) \big(-(n-1)(\delta_2 - \phi_1 - \delta_2\phi_2) - \delta_2(1-\phi) \big) \\
&- 2\phi_1\phi_2 \big(-(n-1)(1-\phi_1-\delta_2\phi_2) - (1-\phi) \big) \big(-(n-1)(\delta_2 - \phi_1 - \delta_2\phi_2) - \delta_2(1-\phi) \big) \\
&+ 4\phi_1\phi_2 \big(-(n-1)(1-\phi_1-\delta_2\phi_2) - \delta_2(1-\phi) \big) \big(-(n-1)(\delta_2 - \phi_1 - \delta_2\phi_2) - (1-\phi) \big).
\end{aligned} \tag{74}$$

To see that $\tilde{I}_2$ is nonnegative, note first that

$$\begin{aligned}
&\big(-(n-1)(1-\phi_1-\delta_2\phi_2) - \delta_2(1-\phi) \big) \big(-(n-1)(\delta_2 - \phi_1 - \delta_2\phi_2) - (1-\phi) \big) \\
&\quad = \big(-(n-1)(1-\phi_1-\delta_2\phi_2) - (1-\phi) \big) \big(-(n-1)(\delta_2 - \phi_1 - \delta_2\phi_2) - \delta_2(1-\phi) \big) \\
&\qquad + (n-1)(1-\delta_2)^2(1-\phi).
\end{aligned} \tag{75}$$

Consequently, we can rewrite $\tilde{I}_2$ as

$$\begin{aligned}
\tilde{I}_2 =& (1-\phi)^2(1-\delta_2)^2 + \phi_1^2 \big(-(n-1)(1-\phi_1-\delta_2\phi_2) - (1-\phi) \big)^2 \\
&+ \phi_2^2 \big(-(n-1)(\delta_2 - \phi_1 - \delta_2\phi_2) - \delta_2(1-\phi) \big)^2 \\
&+ 2\phi_1(1-\delta_2)(1-\phi) \big(-(n-1)(1-\phi_1-\delta_2\phi_2) - (1-\phi) \big) \\
&- 2\phi_2(1-\delta_2)(1-\phi) \big(-(n-1)(\delta_2 - \phi_1 - \delta_2\phi_2) - \delta_2(1-\phi) \big) \\
&+ 2\phi_1\phi_2 \big(-(n-1)(1-\phi_1-\delta_2\phi_2) - (1-\phi) \big) \big(-(n-1)(\delta_2 - \phi_1 - \delta_2\phi_2) - \delta_2(1-\phi) \big) \\
&+ 4\phi_1\phi_2(n-1)(1-\delta_2)^2(1-\phi).
\end{aligned} \tag{76}$$

To proceed, we briefly prove the following inequality, which is written out here first in such a way that the main idea becomes apparent:

$$4\phi_1\phi_2(n-1)(1-\delta_2)^2(1-\phi) \geq 4\phi_2(1-\delta_2)(1-\phi) \big(-(n-1)(\delta_2 - \phi_1 - \delta_2\phi_2) - \delta_2(1-\phi) \big). \tag{77}$$

Obviously, inequality (77) can be reduced to

$$\phi_1(n-1)(1-\delta_2) \geq -(n-1)(\delta_2 - \phi_1 - \delta_2\phi_2) - \delta_2(1-\phi),$$

that is

$$(n-1)\phi_1 - \delta_2 n\phi_1 + \delta_2\phi_1 \geq -(n-1)\delta_2 + (n-1)\phi_1 + \delta_2(n-1)\phi_2 - \delta_2 + \delta_2\phi_1 + \delta_2\phi_2.$$

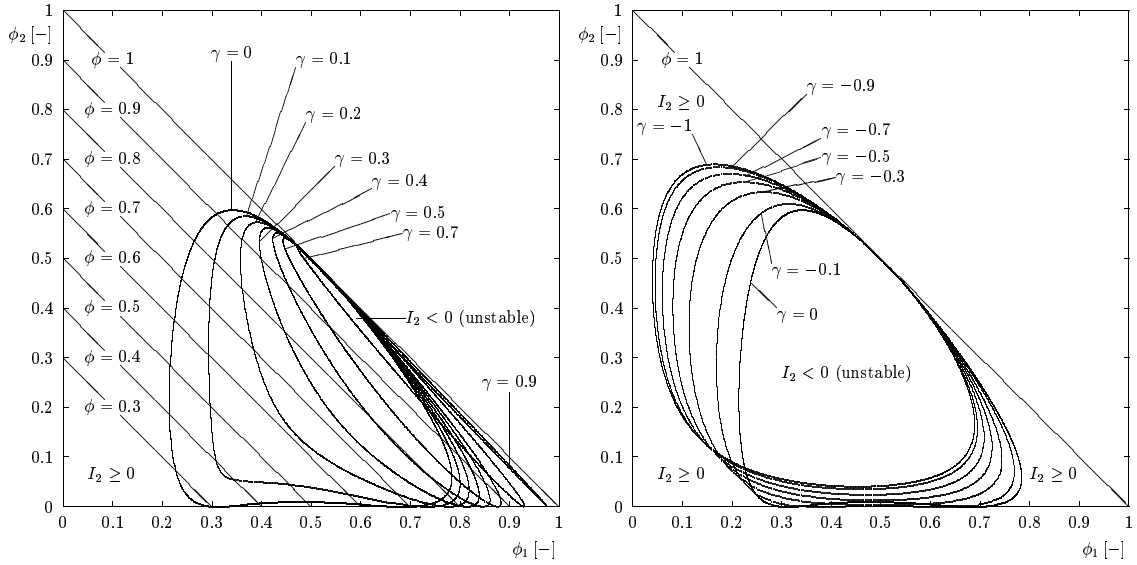

FIGURE 2. Instability regions of the MLB model for $N = 2$ with $n = 4.65$ and particles of the same size and the indicated relative density ratios $\gamma = \bar{\varrho}_2/\bar{\varrho}_1$. The left and right diagrams correspond to bidisperse suspensions with two heavy and one heavy and one buoyant (creaming) particle species, respectively, and include the instability region for the common limiting case $\gamma = 0$.

After cancellations, we get from this $-\delta_2 n\phi_1 \geq -n\delta_2 + n\delta_2\phi_2$, that is $\phi_1 + \phi_2 \leq 1$, which is true on $\mathcal{D}_1$. Therefore (77) holds on $\mathcal{D}_{\phi_{\max}}$ for all $0 < \phi_{\max} \leq 1$. In view of (77), we obtain from (76)

$$\begin{aligned}
\tilde{I}_2 \geq & (1-\phi)^2(1-\delta_2)^2 + \phi_1^2\big(-(n-1)(1-\phi_1-\delta_2\phi_2) - (1-\phi)\big)^2 \\
& + \phi_2^2\big(-(n-1)(\delta_2-\phi_1-\delta_2\phi_2) - \delta_2(1-\phi)\big)^2 \\
& + 2\phi_1(1-\delta_2)(1-\phi)\big(-(n-1)(1-\phi_1-\delta_2\phi_2) - (1-\phi)\big) \\
& + 2\phi_2(1-\delta_2)(1-\phi)\big(-(n-1)(\delta_2-\phi_1-\delta_2\phi_2) - \delta_2(1-\phi)\big) \\
& + 2\phi_1\phi_2\big(-(n-1)(1-\phi_1-\delta_2\phi_2) - (1-\phi)\big)\big(-(n-1)(\delta_2-\phi_1-\delta_2\phi_2) - \delta_2(1-\phi)\big) \\
= & \Big\{(1-\phi)(1-\delta_2) + \phi_1\big(-(n-1)(1-\phi_1-\delta_2\phi_2) - (1-\phi)\big) \\
& \quad + \phi_2\big(-(n-1)(\delta_2-\phi_1-\delta_2\phi_2) - \delta_2(1-\phi)\big)\Big\}^2.
\end{aligned} \tag{78}$$

Thus we have shown that $I_2 = (\mu\bar{\varrho}_2(1-\phi)^{n-2})^2\tilde{I}_2 \geq 0$. Consequently, the MLB model is stable, that is hyperbolic, for bidisperse suspensions of spheres having the same density, for arbitrary size ratios $\lambda_{12} = d_2/d_1 = \sqrt{\delta_2}$ and arbitrary RICHARDSON-ZAKI exponents $n \geq 1$. This general stability result comes from a straightforward computation, while BIESHEUVEL et al. [11] still formulate it as a conjecture motivated from a number of test calculations, and is in agreement with the weight of evidence from numerous experiments that instabilities do not occur in bidisperse suspensions with spheres of the same density but with different sizes. (See Section 6.1.)

We now determine instability regions for the MLB model for bidisperse suspensions of particles of the same size but differing in density, for which the stability region depends only on the ratio $\gamma := \bar{\varrho}_2/\bar{\varrho}_1$. Since the roles of Species 1 and 2 can be interchanged, it is sufficient to consider $\bar{\varrho}_2 < \bar{\varrho}_1$. An analytical evaluation of the instability criterion to detect in which cases instability regions do occur is at least cumbersome in this case. Instead, we present here numerically calculated instability regions for a RICHARDSON-ZAKI exponent $n = 4.65$ and both cases of two heavy

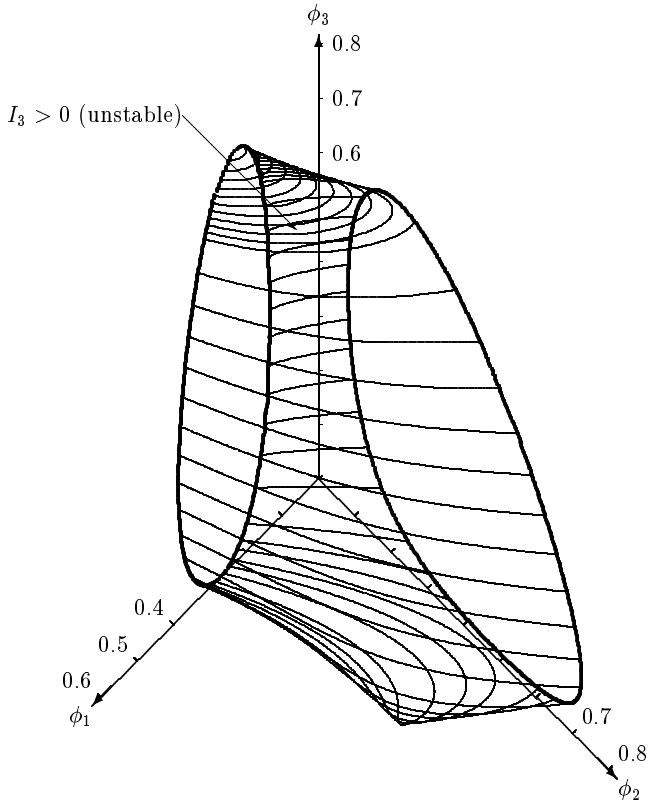

FIGURE 3. Instability region of the MLB model for $N = 3$ with $n = 4.65$, the particle size ratios $d_2/d_1 = d_3/d_1 = 0.5$, and the reduced density ratios $\bar{\varrho}_2/\bar{\varrho}_1 = 1$ and $\bar{\varrho}_3/\bar{\varrho}_1 = -1/2$, constructed by numerical evaluation of condition (70). The thin lines correspond to $\phi_3 = 0.001, 0.005, 0.01, 0.02, 0.03, 0.05, 0.1, \ldots, 0.65, 0.66, 0.67, \ldots, 0.75$. The intersections with the planes $\phi_1 = 0$ and $\phi_2 = 0$ are plotted in fat dots.

($\gamma > 0$) and one heavy and one buoyant (creaming) ($\gamma < 0$) particle species, see Figure 2. Some of the curves forming the contours of the instability regions in both cases have already been shown by BIESHEUVEL et al. [11], but are plotted here on the entire domain $\mathcal{D}_1$, while the plots in [11] are limited to $0 \leq \phi_1, \phi_2 \leq 0.4$. The left diagram of Figure 2 shows that for ratios γ between 0.3 and 1.0, the instability region is located between the lines $\phi = 0.7$ and $\phi = 1$. However, since the spheres are of equal size, the maximum cumulative solids concentration that has to be considered in the bidisperse system is the dense packing volume fraction of around $\phi_{\max} = 0.66$ if the spheres are assumed to be rigid. Thus the instability regions predicted in these cases are not of practical relevance when the MLB model is employed for computations, in which the fluxes would be cut at $\phi = \phi_{\max}$. Such a consideration does not apply to the case $\gamma < 0$, since there always persists an appreciable instability region, except for relatively dilute suspensions with ϕ roughly being smaller than 0.2.

We have also computed and plotted in both diagrams of Figure 2 the common limiting instability region for both cases attained for $\gamma = 0$. Observe that the MLB model produces a large zone of instability for a bidisperse suspension of heavy and neutrally buoyant spheres.

For tridisperse suspensions of particles of the same density but different sizes we have found no pairs of density ratios d_2/d_1 and d_3/d_1 and exponents n that would produce an instability region. A natural conjecture is that the MLB equations are also stable for $N = 3$. To prove this one would have to write out and try to rearrange all terms occurring in I_3, which we do not undertake here.

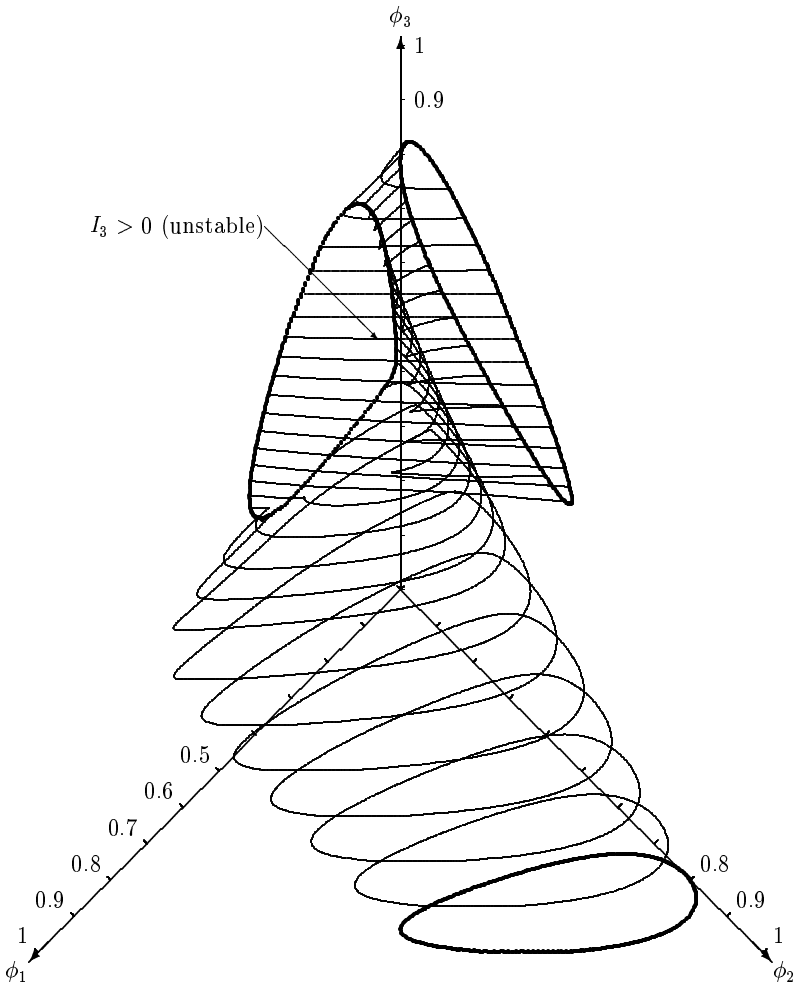

FIGURE 4. Instability region of the MLB model for $N = 3$ with $n = 4.65$, the particle size ratios $d_2/d_1 = 1/\sqrt{2}$, $d_3/d_1 = 0.5$, and the reduced density ratios $\bar{\varrho}_2/\bar{\varrho}_1 = 2$ and $\bar{\varrho}_3/\bar{\varrho}_1 = 4$, constructed by numerical evaluation of condition (70). The thin lines correspond to $\phi_3 = 0.05, 0.1, \ldots, 0.35, 0.375, \ldots, 0.825, 0.85$. The intersections with the planes $\phi_1 = 0$, $\phi_2 = 0$ and $\phi_3 = 0$ are plotted in fat dots.

Instead, we present three numerical evaluations of I_3 in cases where instabilities do exist, which is ensured if different solid densities are present and, of course, $\phi_{\max}$ is large enough.

In Figure 3, we consider the MLB model for $N = 3$ with $n = 4.65$, the particle size ratios $d_2/d_1 = d_3/d_1 = 0.5$, and the reduced density ratios $\bar{\varrho}_2/\bar{\varrho}_1 = 1$ and $\bar{\varrho}_3/\bar{\varrho}_1 = -1/2$. As expected, the instability region, which is roughly an interpolation between the two bidisperse instability regions, avoids the plane $\phi_3 = 0$. However, Figure 3 predicts that adding only 0.1% of volume of buoyant particles (of Species 3) provokes instability for a large region of pairs (ϕ_1, ϕ_2), e.g. $\phi_1 = 0.2$, $\phi_2 = 0.15$, of the concentrations of a stable bidisperse suspension.

The different roles of particle sizes and densities in the MLB equations have already been demonstrated in [11] for the case $N = 2$. We consider in Figure 4 the MLB model for $N = 3$ with $n = 4.65$, the particle size ratios $d_2/d_1 = 1/\sqrt{2}$, $d_3/d_1 = 0.5$, and the reduced density ratios $\bar{\varrho}_2/\bar{\varrho}_1 = 2$ and $\bar{\varrho}_3/\bar{\varrho}_1 = 4$. Note that in view of (32), the three particle species share the same Stokes velocity $\mathbf{u}_\infty$. Thus monodisperse suspensions of each of these species will behave identically given the same initial and boundary conditions. However, the tridisperse suspension has a relatively complex instability region.

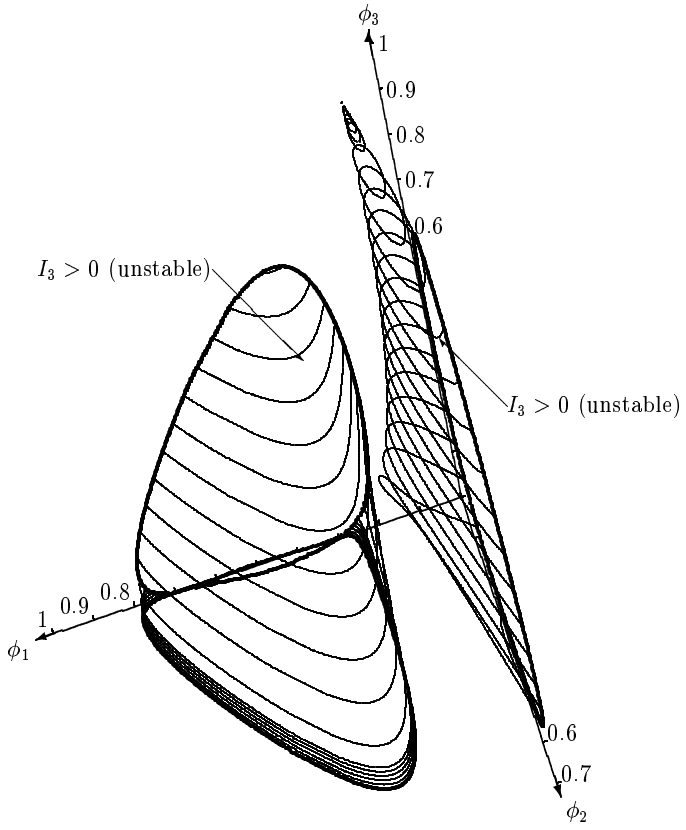

FIGURE 5. Instability region of the MLB model for $N = 3$ with $n = 4.65$, identical particle sizes, and the reduced density ratios $\bar{\varrho}_2/\bar{\varrho}_1 = 0.05$ and $\bar{\varrho}_3/\bar{\varrho}_1 = -0.05$, constructed by numerical evaluation of condition (70). The thin lines correspond to $\phi_3 = 0.005, 0.01, \ldots, 0.025, 0.05, 0.1, \ldots, 0.85, 0.86, \ldots, 0.92$. The intersections with the planes $\phi_1 = 0$, $\phi_2 = 0$ and $\phi_3 = 0$ are plotted in fat dots.

In the case $N = 3$, the instability region can take a very complex shape and need not be one connected subdomain of $\mathcal{D}_{\phi_{\max}}$. This is illustrated in Figure 5, where we consider identical particle sizes, and $\bar{\varrho}_2/\bar{\varrho}_1 = 0.05$ and $\bar{\varrho}_3/\bar{\varrho}_1 = -0.05$. In this case, the instability region decomposes into two disconnected domains. The coordinate axes in Figure 5 have been slightly inclined to make this visible. We have, of course, checked many more levels of $\phi_3 = const.$ such that it is ensured that these domains are indeed disconnected.

5.2. **Stability of the modifications of** BATCHELOR**'s equations.** The partial derivatives of the flux vector of the DG model defined by (52) are

$$\begin{aligned}\frac{\partial f_i^{\mathrm{DG}}(\Phi)}{\partial \phi_k} = \mu \bar{\varrho}_{\mathrm{s}} \delta_i (1-\phi)^{-S_{ii}} \Big[\big(1 + \mathbf{e}_i^{\mathrm{T}} \mathbf{S} \Phi - \phi S_{ii}\big)\delta_{ik} \\ + \phi_i \left(S_{ik} + \frac{S_{ii}}{1-\phi} \big(\phi + \mathbf{e}_i^{\mathrm{T}} \mathbf{S} \Phi - \phi S_{ii}\big) \right) \Big], \quad 1 \le i, k \le N. \end{aligned} \tag{79}$$

We first consider the bidisperse case and show that if the matrix $\mathbf{S}$ is given by formula (49), then the DAVIS and GECOL model is stable provided that the number λ_{12} (and hence $\lambda_{21} = \lambda_{12}^{-1}$) are close enough to one, i.e. if the particles do not differ too much in diameter.

To prove that a bidisperse suspension is stable, it is sufficient to show that

$$\frac{\partial f_1(\phi_1, \phi_2)}{\partial \phi_2} \frac{\partial f_2(\phi_1, \phi_2)}{\partial \phi_1} > 0, \tag{80}$$

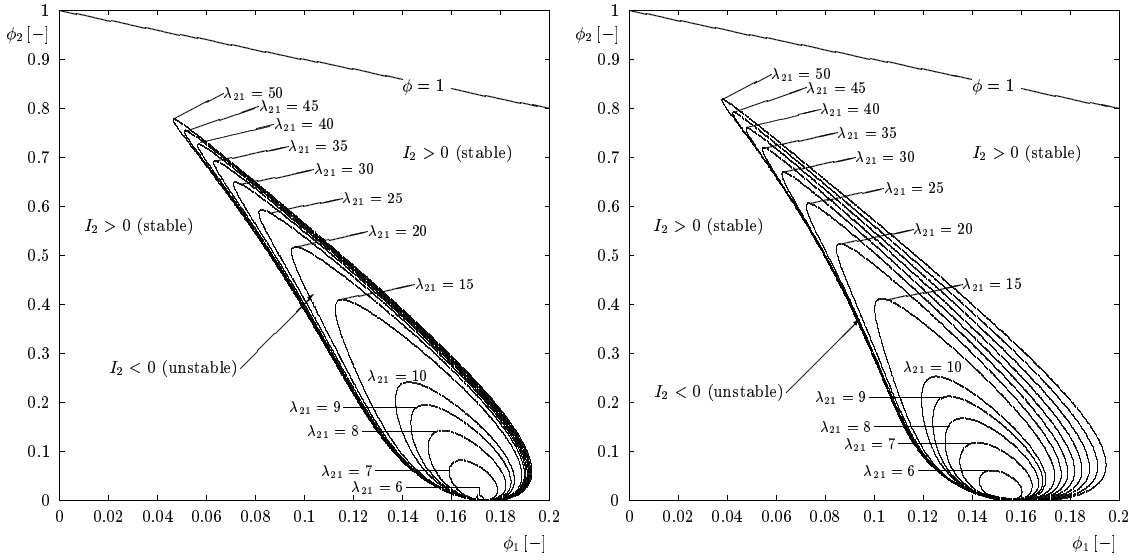

FIGURE 6. Instability regions for $N = 2$ and the indicated particle size ratios $\lambda_{21} = d_1/d_2 = 1/\sqrt{\delta_2}$ of the DG model, constructed by numerical evaluation of condition (60). The left and right diagrams correspond to the parameter vectors (50) and (51), respectively, determined by DAVIS and GECOL [25]. The tested values $\lambda_{21} = 1, 2, \ldots, 5$ do not produce an instability region.

because it then follows from (60) that $I_2 > 0$. In fact, we here get

$$\begin{aligned}\frac{\partial f_1^{\mathrm{DG}}}{\partial \phi_2}\frac{\partial f_2^{\mathrm{DG}}}{\partial \phi_1} = \big(\mu \bar{\varrho}_{\mathrm{s}}(1-\phi)^{-S_{11}}\big)^2 \delta_2 \phi_1 \phi_2 \bigg[S_{12}S_{21} + \frac{S_{12}S_{11}}{1-\phi}\big(\phi + (S_{21}-S_{11})\phi_2\big) \\ + \frac{S_{21}S_{11}}{1-\phi}\big(\phi + (S_{12}-S_{11})\phi_1\big) + \left(\frac{S_{11}}{1-\phi}\right)^2 \big(\phi + (S_{12}-S_{11})\phi_1\big)\big(\phi + (S_{21}-S_{11})\phi_2\big)\bigg].\end{aligned} \tag{81}$$

Note that by (49), we always have $S_{ij} \le S_{ii}$ for $1 \le j < i \le N$ for arbitrary N. Consequently, the four summands in the square brackets of (81) are all positive if

$$\phi + (S_{21} - S_{11})\phi_2 = \phi_1 + \big[1 + (S_{21} - S_{11})\big]\phi_2 \ge 0 \quad \text{for all } (\phi_1, \phi_2) \in \mathcal{D}_1.$$

This condition is indeed satisfied if

$$|S_{21} - S_{11}| = \big|\beta_1(\lambda_{21} - 1) + \beta_2(\lambda_{21}^2 - 1) + \beta_3(\lambda_{21}^3 - 1)\big| \le 1, \tag{82}$$

which is valid if the size ratio λ_{21} is sufficiently close to one. This condition is a sufficient condition for the DG model to be stable. For a precise determination of the stability region in terms of λ_{21} for given parameter values it is necessary to evaluate the full instability criterion (60).

To demonstrate that the DG model with the parameters given in [25] becomes unstable in a subregion of $\mathcal{D}_1$ when λ_{21} becomes large, that is when the squared size ratio δ_2 becomes small, we evaluated the quantity I_2 numerically, using the parameter vectors (50) and (51), respectively, and the test values of the size ratio $\lambda_{21} = 1/\sqrt{\delta_2} = 1, 2, \ldots, 9, 10, 15, 20, \ldots, 50$. Figure 6 shows that for both parameter vectors $\boldsymbol{\beta}$, there exist instability regions in the (ϕ_1, ϕ_2)-plane where $I_2 < 0$, i.e. where the system changes from hyperbolic to elliptic type. Moreover, we see that the size of the instability region increases as λ_{21} does. Furthermore, the smallest value λ_{21} producing an instability region lies in both cases between 5 and 6 (5.868 and 5.070 for the parameter vectors (50) and (51), respectively).

Particular attention is drawn to the limit $\phi_2 \to 0$, for which $\partial f_2^{\mathrm{DG}}/\partial \phi_1(\phi_1, \phi_2) \to 0$ and hence $I_2 \ge 0$. To examine the lower boundary of the region of instability, we set $\phi_2 = 0$ and calculate

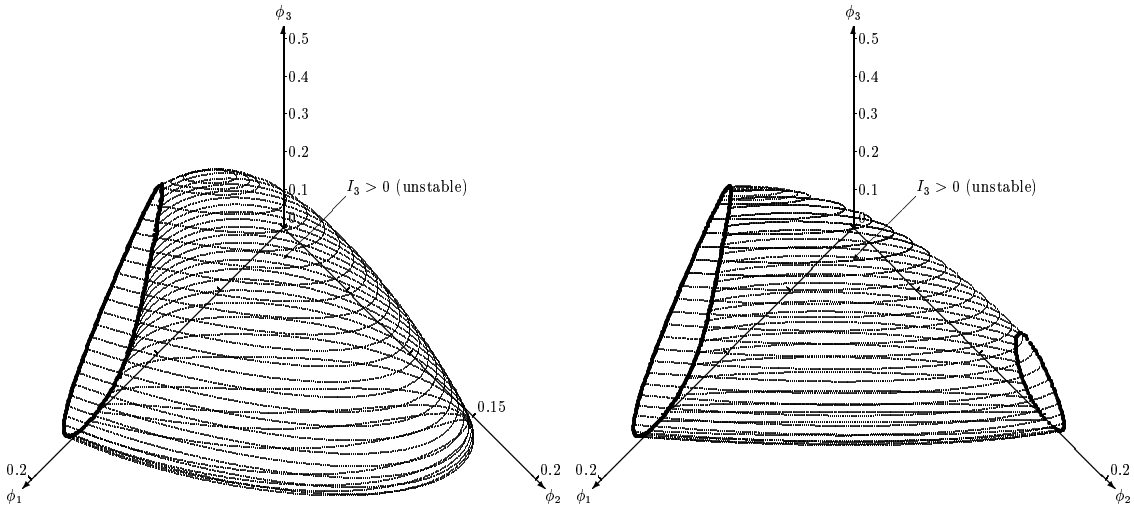

FIGURE 7. Instability regions of the DG model with parameter vector (51), for $N = 3$ and the particle size ratios $\lambda_{21} = d_1/d_2 = 4$ and $\lambda_{32} = d_2/d_3 = 4$ (left) and $\lambda_{21} = 2$ and $\lambda_{32} = 8$ (right), constructed by numerical evaluation of condition (70). The thin lines correspond to $\phi_3 = 0.001, 0.005, 0.01, 0.02, 0.04, \ldots, 0.44, 0.445, 0.45, 0.455$ in the left and $\phi_3 = 0.001, 0.005, 0.01, 0.02, 0.04, \ldots, 0.42, 0.425, 0.43, 0.435$ in the right diagram. The intersections with the planes $\phi_1 = 0$ and $\phi_2 = 0$ are plotted in fat dots.

values of $\phi_1 = \phi$ such that $\partial f_1^{\mathrm{DG}}/\partial\phi_1 = \partial f_2^{\mathrm{DG}}/\partial\phi_2$. This will be true whenever

$$1 + \frac{S_{11}\phi}{1-\phi} = \delta_2\big(1 + (S_{21} - S_{11})\phi\big).$$

This yields a quadratic equation in ϕ,

$$(S_{11} - S_{21})\phi^2 + \big(\lambda_{21}^2(1 - S_{11}) - (S_{11} - S_{21} + 1)\big)\phi + 1 - \lambda_{21}^2 = 0, \tag{83}$$

which has two real roots, one positive and one negative. The positive root yields the values $\phi_1 = \phi_1^*$ for which $I_2 = 0$. Some of them are given in the following table, where the Batchelor matrix $\mathbf{S}$ has been computed with the coefficients given by either (50) or (51):

λ_{21}	2	3	4	5	6	7	8	10	50
ϕ_1^* (Eq. (50))	0.1371	0.1605	0.1678	0.1709	0.1725	0.1733	0.1738	0.1743	0.1760
ϕ_1^* (Eq. (51))	0.1223	0.1417	0.1507	0.1534	0.1547	0.1549	0.1559	0.1565	0.1661

Note that the positive roots occur for $\lambda_{21} = 2, \ldots, 5$, for which uniformly $I_2 \geq 0$ on $\mathcal{D}_1$ as well as for the values plotted in Figure 6 ($\lambda_{21} = 1$ yields only the trivial value $\phi_1 = 0$). This means that even in stable cases the two real eigenvalues coincide at $(\phi_1^*, 0)$.

The results of this analysis are remarkable in that DAVIS and GECOL [25, 26] explicitly recommend the use of their hindered settling function with these parameters for size ratios up to $\lambda_{21} = 8$, but state that it does *not* apply for suspensions in which lateral segregation takes place. However, with the present analysis, their hindered settling function may potentially predict unstable behaviour. DAVIS and GECOL finish their paper [25] with a reference to BATCHELOR and JANSE VAN RENSBURG's stability analysis [5], but unfortunately do not apply it.

In the case $N = 3$, a similar simplified stability analysis in terms of the density ratios occurring is not possible, since the model equations are stable if $I_3 < 0$ on $\mathcal{D}_1$, which requires evaluating both p and q, while to show instability, it is sufficient to consider the quantity p only. For the reasons discussed towards the end of Section 4, we expect three-dimensional instability regions to exist wherever two of the particle species possess a density ratio larger than about six.

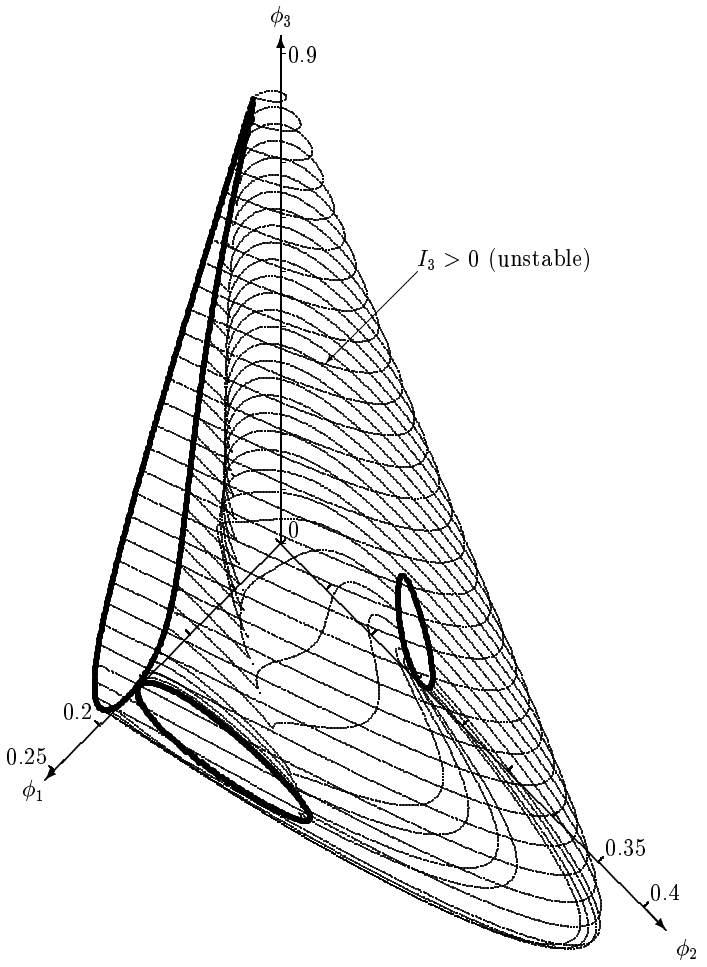

FIGURE 8. Instability region of the DG model with parameter vector (51), for $N = 3$ and the particle size ratios $\lambda_{21} = d_1/d_2 = 8$ and $\lambda_{32} = d_2/d_3 = 8$, constructed by numerical evaluation of condition (70). The thin lines correspond to $\phi_3 = 0.005, 0.01, 0.02, 0.03, 0.06, \ldots, 0.9$. The intersections with the planes $\phi_1 = 0$, $\phi_2 = 0$ and $\phi_3 = 0$ are plotted in fat dots.

We illustrate this observation by a numerical evaluation of the instability condition (70) for $N = 3$. We select the parameter vector (51) and consider first the size ratios $\lambda_{21} = d_1/d_2 = 4$ and $\lambda_{32} = d_2/d_3 = 4$. Here all states Φ with $\phi_3 = 0$ or $\phi_1 = 0$ are stable, since (according to Figure 6) the corresponding size ratio of 4 in both cases does not fall within the bidisperse instability region. However, wherever $\phi_2 = 0$ the remaining Species 1 and 3 form a bidisperse suspension with size ratio 16, which does produce an instability region. Consequently, the three-dimensional tridisperse instability region will not intersect the planes $\phi_1 = 0$ or $\phi_3 = 0$, and its intersection with $\phi_2 = 0$ will be identical to the instability region for $N = 2$ with $\lambda_{21} = 16$. The left diagram of Figure 7 displays the numerical instability region in this situation.

If we assume the size ratios $\lambda_{21} = 2$ and $\lambda_{32} = 8$, also the plane $\phi_1 = 0$, corresponding to a bidisperse suspension with size ratio 8, will have a nonempty intersection with the three-dimensional instability region.

Finally, we consider the case $\lambda_{21} = 8$ and $\lambda_{32} = 8$, in which we expect nonempty intersections with all three planes $\phi_1 = 0$, $\phi_2 = 0$ and $\phi_3 = 0$. The corresponding three-dimensional instability region is plotted in Figure 8. Observe that the volume of the instability region is surprisingly much larger than one would expect given the relatively small area occupied by each of the three

two-dimensional instability regions in its respective coordinate plane. Note that the shape of cross-sectional area of the instability region (with respect to height) changes rapidly as soon as ϕ_3 starts to take positive values. For example, the point $\Phi = (0.05, 0.35, 0)$ is clearly stable. However, the point $\Phi = (0.05, 0.35, 0.005)$ is not, which means that the DG model with the given parameters predicts that adding only 0.5% volume fraction of a small particles to a stable suspension of spheres that are eight and 64 times larger can produce instability.

It should be emphasized that it is not claimed here that this does actually happen in polydisperse sedimentation. Rather, our study is aimed at evaluating models for polydisperse sedimentation, as given by the variety of flux density vectors proposed in the literature, by means of mathematical analysis and linear algebra. In this case we have demonstrated the consequences of the innocent use of DAVIS and GECOL's hindered settling functions in a situation it clearly was not designed for, since the maximum size ratio in the tridisperse system just considered is 64.

We finally briefly consider the HS model, which has not been studied as extensively as the MLB and DG models. For the flux density vector introduced in Eq. (54), we obtain

$$\frac{\partial f_i^{\mathrm{HS}}(\Phi)}{\partial \phi_k} = \mu \bar{\varrho}_{\mathrm{s}} \delta_i \left(1-\bar{\phi}\right)^n \exp\left(\mathbf{e}_i^{\mathrm{T}} \mathbf{S} \Phi + n\bar{\phi}\right) \left[\delta_{ik} + \left(S_{ik} - \frac{n}{\phi_{\max}} \frac{\bar{\phi}}{1-\bar{\phi}}\right)\phi_i\right], \quad 1 \le i,k \le N. \quad (84)$$

It is easy to see that the HS model is stable for $N = 2$ and Batchelor matrices $\mathbf{S}$ with arbitrary nonpositive entries. Indeed, (80) is true on $\mathcal{D}_1$, since

$$\left(S_{12} - \frac{n}{\phi_{\max}} \frac{\bar{\phi}}{1-\bar{\phi}}\right)\left(S_{21} - \frac{n}{\phi_{\max}} \frac{\bar{\phi}}{1-\bar{\phi}}\right) > 0$$

due to assumptions (49). We have not found size ratios for tridisperse suspensions in which the HS model would be unstable and thus conjecture that it is stable also for $N = 3$, as is the MLB model.

6. DISCUSSION

6.1. **Comparison with numerical and experimental results.** REVAY and HIGDON [58] used Stokesian dynamics [13] to study the sedimentation of bidisperse suspensions in which the spheres differed only in density. The contour for $\gamma = -1$ in our Figure 2 is fairly close to the computed result shown in their Figure 8 and very close to the experimental results of FESSAS and WEILAND [29] that are also shown in that figure. For $\gamma > 0$, there is qualitative agreement that instability exists at low values, but not at high. For the MLB model, only the instability contours for 0.1 and 0.2 lie within the range of feasible concentrations; REVAY and HIGDON predict instability for $\gamma \le 0.39$. Their contours lie to the left of ours and are closer together.

FESSAS and WEILAND [29] provide a vivid description of experimental instability: *"... the initially uniform mixture immediately became grainy and large clusters containing predominately heavy or light particles formed. These clusters moved up or down, depending on composition, colliding and interacting with each other. In doing so, the heavy (dark) clusters, for example, ejected whatever buoyant (yellow) particles they contained. It seemed that a large proportion of the overall settling took place by the rapid ascent and descent of clusters containing virtually one particulate phase only."* A sequence of small photographs in WEILAND et al. [71] shows all of the stages in this kind of separation. Figure 2 of LAW et al. [47] illustrates the different appearance of stable and unstable systems: their Figure 2(a) shows stable behaviour, similar to our schematic illustration Fig. 1(a), for initial concentrations $\Phi_1^0 = (\phi_1^0, \phi_2^0) = (0.08, 0.08)$, while instabilities are clearly visible in their Figure 2(b) at $\Phi_2^0 = (0.2, 0.15)$. LAW et al. [47] indicated that the RICHARDSON-ZAKI exponent $n = 5.39$ was suitable for their spheres, and indeed their observations of stable and unstable behaviour at different initial concentrations are consistent with the instability region produced by the MLB model with this value of n and the appropriate densities, see Figure 9. As discussed below, instability phenomena in the second case could however not be reproduced numerically in [17].

Delineation of the boundaries of experimental instability is difficult. A grainy appearance and a fingering flow structure are usually considered to indicate instability, even in the absence of the dramatic developments noted above. Table 1 of BATCHELOR and JANSE VAN RENSBURG [5] lists

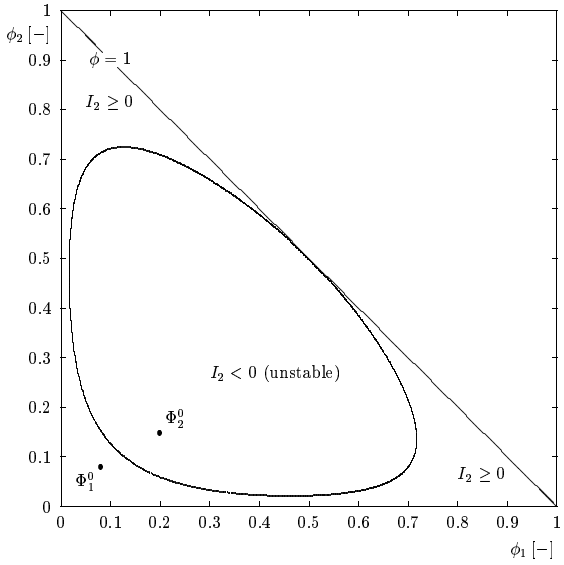

FIGURE 9. Instability region of the MLB model for $N = 2$ with $n = 5.39$ and equal-sized particles with the densities $\varrho_1 = 1186\,\mathrm{kg/m^3}$ and $\varrho_2 = 1050\,\mathrm{kg/m^3}$, where $\varrho_\mathrm{f} = 1120\,\mathrm{kg/m^3}$, according to LAW et al. [47]. The points $\Phi_1^0 = (0.08, 0.08)$ and $\Phi_2^0 = (0.2, 0.15)$ correspond to both the experiments by LAW et al. [47] and the computations by BÜRGER et al. [17, Figs. 8–13].

the properties of particles and fluid for systems in which streaming columns have been observed. With one exception ($\gamma = 1$, $\lambda_{12} = 0.63$), these are in general agreement with our Figure 2. This exception, which appears as Figure 3 of WEILAND et al. [71], is almost certainly not a true case of $I_2 < 0$. As noted by BIESHEUVEL et al. [11], many authors who have studied cases where $\gamma = 1$ have never reported instabilities and have explicitly mentioned stable sedimentation. Clusters form and columns of spheres move upward and downward to some extent even in monodisperse suspensions [65], and occasionally these currents are surprisingly strong. Though these features are usually not pronounced in stable bidisperse suspensions, they are sometimes not easily distinguished from marginal instability. On the other hand, BATCHELOR and JANSE VAN RENSBURG's Figure 7 indicates that suspensions with $\lambda_{12} \approx 1$ and $\gamma \leq 0.5$ are unstable when $\phi_1 = \phi_2 = 0.15$. Stokesian dynamics [58, Figure 7] and the MLB model predict stability for all $\gamma \geq 0$ at these concentrations (as shown in our Figure 2 and Figure 5 of BIESHEUVEL et al. [11]). These authors and YAN and MASLIYAH [72] provide many comparisons of the MLB (Masliyah) model with experimental data for bidisperse systems.

6.2. **Mixed systems of conservation laws.** The analysis in this paper shows that commonly used polydisperse sedimentation models give rise to systems of conservation laws which contain regions of the phase space where the systems are non-hyperbolic (elliptic for $N = 2$). Such systems are frequently referred to as *mixed* systems of conservation laws. In addition to the application considered in this contribution, such mixed systems occur in variety of applications including transonic flow, traffic flow, one-dimensional unsteady flow of a van der Waals gas, propagation of phase boundaries in elastic bars, enhanced oil recovery and multiphase (water, gas, oil) flow in porous media, inertia-free shear-thinning flow, and two-phase flow. Of particular interest in the light of the present analysis are systems of conservation laws modeling three-phase flow in porous media, since there are some similarities to the systems modeling polydisperse sedimentation.

In fact, models for multiphase flow in porous media formed the main stimulus for intense research related to systems that change type. We refer to [31, 43, 44, 49, 50] for overviews of the theory of mixed systems of conservation laws and their applications. Following [31, 43, 44, 49, 50],

we shall here only briefly review some of the current views that exist today regarding mathematical and numerical theory for these mixed systems.

An obvious question arising from elliptic regions is that of the actual effect of the appearance of complex eigenvalues. First of all, in practical numerical calculations, the existence of elliptic regions does not appear to introduce computational instabilities, which is why the change of type was not noticed at first [7]. Here it is appropriate to mention that oscillations were not observed in the numerical calculations performed in [17] for various systems of conservation laws modeling polydisperse sedimentation. In particular, the simulation of both the stable and unstable cases depicted in Figure 9 (corresponding to the experiments by LAW et al. [47]) turned out to be free of oscillations. (With the present analysis, it is clear that the two 2×2 systems, of the MLB and HS models, solved in our second paper [18] are both hyperbolic.)

One reason for the lack of oscillations is, of course, the numerical diffusion introduced by most numerical schemes, which turns the system of conservation laws into a parabolic system, which is well-posed (see below). Nevertheless, the existence of oscillatory solutions (which are measure-valued solutions) for non-hyperbolic systems has been proved both analytically and numerically [33]. In fact, the numerical study [34] (using a first-order finite difference scheme) of the solution to Riemann problems with initial data inside elliptic regions revealed that approximate solutions may present persistent large amplitude oscillations. Numerical studies have also shown that, when one state belongs to the hyperbolic region and the other to the elliptic, the solution is acceptable, but still displays some oscillations. On the other hand, when both states are located in the hyperbolic region, the numerical solutions seems to be stable. It has furthermore been demonstrated that solutions to Riemann problems with 'hyperbolic' initial data avoid the elliptic regions, which is a potentially interesting result. The distinction between Riemann and more general Cauchy problems is essential, since this avoidance of the elliptic region is not true for more general Cauchy data [38, 56].

Although solutions of Riemann problems may display oscillations, a view advocated in, e.g., [43, 44] is that for general Cauchy data (not Riemann data) nonlinear wave interactions remove the catastrophic high-frequency ill-posedness (in the sense of Hadamard) associated with linear mixed systems. In a nonlinear system, the instability does not grow exponentially (as in the linear non-hyperbolic case), but saturates. This means that once the solution takes values in the hyperbolic region, it stops growing. In fact, in practical examples there is no evidence of catastrophic failure of well-posedness of the general Cauchy problem. It seems that systems that change type appear to be incomplete rather than catastrophically ill-posed [43, 44]. But we know already that hyperbolic models are incomplete in the sense that shock admissibility criteria are needed to make the models well-posed. It can be expected that the solution of mixed systems is more sensitive to the choice of admissibility criteria than is the solution of hyperbolic systems.

Although it outside the scope of this paper go into details about admissibility criteria, we mention that there are three dominating shock admissibility criteria presently in use: linearized stability, viscous profile, and nonlinear stability. In particular, the viscous profile approach has been popular, which essentially consists of adding an (artificial or physical) diffusion term $(\partial/\partial x)(\mathbf{D}(\Phi)(\partial\Phi/\partial x))$ to the right-hand side of (2) and then looking at traveling-waves solutions to the resulting convection-diffusion system. Here $\mathbf{D}(\Phi)$ is the diffusion matrix and "artificial diffusion" refers to the choice $\mathbf{D} = \varepsilon\mathbf{I}$ for some small constant $\varepsilon > 0$. For example, in most finite difference schemes the (numerical) diffusion is a polynomial in $\mathcal{J}_{\mathbf{f}}(\Phi)$. There are examples of systems where the viscous profile criterion is insufficient to ensure uniqueness of the Riemann solutions, although it includes and generalizes the other well-known entropy conditions (see [3, 49, 50], and the references therein).

One such example is given by the mixed systems of conservation laws modeling immiscible three-phase flow of water, gas, and oil in porous media (which usually contain elliptic regions) [7]. Similar to the polydisperse sedimentation models, three-phase flow models (when capillary effects are ignored) are based on the mass conservation principle for each phase along with constitutive assumptions such as Darcy's law and empirical expressions for determining the three-phase relative permeabilities as functions of the saturations of the phases. If the capillary pressure is taken into

account, then the convection system becomes a convection-diffusion system with a (physical) capillary diffusion matrix $\mathbf{D}$ (which we do not detail here).

As already mentioned, solutions of Riemann problems (with 'elliptic' data) display large-amplitude rapid oscillations. In earlier times, there seems to have been a general opinion that conservation laws should yield a satisfactory hyperbolic theory outside the elliptic region. However, recent work emphasizes a more primary reason for anomalous behavior: namely, *linearized instability* of the full convection-diffusion system, rather than ill-posedness of the purely convection system (see [3] and the references therein). These two concepts coincide when the artificial diffusion $\mathbf{D}(\Phi) = \varepsilon \mathbf{I}$, or more generally when convective and diffusive effects commute (which is the case in most finite difference schemes). On the other hand, MAJDA and PEGO [52] show that the structure of the diffusion matrix $\mathbf{D}$ is important when other (nonlinear) diffusion matrices are considered. They develop a useful sufficient condition in terms of $\mathbf{D}$ and $\mathcal{J}_{\mathbf{f}}$ for linearized instability. The corresponding Majda-Pego instability region contains but is typically larger than the ellipticity region, see [3]. Non-uniqueness or nonexistence of solutions to Riemann problems (the latter manifests itself in terms of highly oscillatory measure-valued solutions) can occur in the Majda-Pego instability region, even in zones of strict hyperbolicity. In particular, so-called non-classical *transitional* shock waves occur generically in models for three-phase flow in porous media. A transitional shock wave is sensitive to diffusion and hence it seems that capillary pressure must be modeled correctly to calculate the flow [49]. The fact that transitional shock waves are sensitive to the precise form of the diffusion matrix does not mean that they are unstable solutions. However, since transitional shock waves cannot be determined without specifying the diffusion, the systems that govern three-phase flow are physically and mathematically ill-defined in the absence of capillary pressure. Furthermore, the same fact implies that numerical simulation by standard hyperbolic difference schemes of flow containing such waves can be misleading. The computed transitional shock wave, and therefore the overall solution, can be associated with numerical diffusion instead of the physical capillary diffusion. On the other hand, numerical schemes that resolve the parabolic system capture these effects.

To regard a system that changes type as an inviscid limit of a parabolic system is not entirely satisfactory since, as was discussed above, the stability or admissibility of such shock waves may depend on the form of the (nonlinear) diffusion matrices. For example, it is not clear what the physical diffusion matrix should look like for the polydisperse sedimentation models studied here, but computational and experimental studies of hydrodynamic diffusion [18, 24, 39, 46, 63] in polydisperse suspensions may offer guidance. This system is radically different from the three-phase flow systems for which the capillary pressure model provides the correct form of the diffusion matrix. Consequently, in view of the above discussion, it seems unlikely that the viscous profile criterion will turn out to be useful in the study of shock waves for mixed systems of conservation laws modeling polydisperse sedimentation. This motivates the search for "inviscid" stability criteria for shocks in mixed systems of conservation laws. It is outside the scope of this work go into details about this, but refer to [43] and the references therein.

Summarizing, it can be stated that the mathematical and numerical theory as well as the general understanding of mixed systems has advanced significantly since mixed systems were first observed in applications [7]. However, most essential problems have remained unsolved. In particular, there exists no core theory and there is no general agreement on admissibility criteria for mixed systems.

Finally, we emphasize that the complicated shock wave structures [43, 44, 49, 50] that are seen in the solutions of mixed systems are usually not observed experimentally. In the absence of practical evidence, one is of course led to conclude that the main reason that mixed systems occur is inappropriate modeling (mixed nature arises often from closure laws). This sharply contrasts with the mixed systems studied in this paper. In fact, we have demonstrated that the occurrence of elliptic regions is the origin of some of the unstable modes that clearly have been observed experimentally, as discussed in Section 6.1.

Acknowledgements

The preparation of this paper was made possible by support from the European Science Foundation (ESF) through the Applied Mathematics in Industrial Flow Problems (AMIF) programme. Support by the Sonderforschungsbereich 404 at the University of Stuttgart is also gratefully acknowledged. This work was done while Karlsen was visiting the Institute for Pure and Applied Mathematics (IPAM), at the University of California, Los Angeles (UCLA). He is grateful to IPAM for their hospitality and support.

Appendix: Equivalence of surface and volume porosities

Consider a polydisperse suspension of spheres sedimenting in a container of constant cross-sectional area. Let $a_i(z,t)$ be the fraction of that area occupied by the ith species ($i = 1, \dots, N$) at height z and time t. Then a_i is non-negative and continuous, but not smooth [57]. The volume fraction of the ith species in a region of height L is

$$\phi_i(t) = \frac{1}{L}\int_0^L a_i(z,t)\,dz.$$

If $a_i(z,t)$ is stochastically stationary with z,

$$\mathcal{E}\big(\phi_i(t)\big) = \frac{1}{L}\mathcal{E}\left(\int_0^L a_i(z,t)\,dz\right) = \frac{1}{L}\int_0^L \mathcal{E}\big(a_i(t)\big)\,dz$$

by Fubini's theorem [21]. Thus $\mathcal{E}(\phi_i(t)) = \mathcal{E}(a_i(t))$ and $\mathcal{E}(\phi(t)) = \mathcal{E}(a(t))$, where $a := a_1 + \cdots + a_N = 1 - \epsilon$. Thus the surface and volume porosities are equal whenever they are stochastically stationary. (This proof, which follows Blum's treatment [12], can be generalized to arbitrary particles. In this case, a_i has at most a finite number of small discontinuities [57] and therefore is integrable.)

Since we are not concerned with small random fluctuations, we take $\phi_i(t) = \mathcal{E}\big(\phi_i(t)\big)$. Thus, it is natural to take

$$\phi_i(z,t) = \lim_{h\to 0}\frac{1}{2h}\int_{z-h}^{z+h}\mathcal{E}\big(a_i(\zeta,t)\big)\,d\zeta = \mathcal{E}\big(a_i(z,t)\big)$$

whenever the latter varies smoothly.

References

[1] Arastoopour,H.; Lin, S.C.; Weil, S.A.: Analysis of vertical pneumatic conveying of solids using multiphase flow models. AIChE J. **28** (1982), 467–473.

[2] Austin, L.G.; Lee, C.H.; Concha, F.; Luckie, P.T.: Hindered settling and classification partition curves. Minerals & Metallurgical Process. **9** (1992), 161–168.

[3] Azevedo, A.V.; Marchesin, D.; Plohr, B.; Zumbrun, K.: Capillary instability in models for three-phase flow. Z. Angew. Math. Phys., to appear.

[4] Batchelor, G.K.: Sedimentation in a dilute polydisperse system of interacting spheres. Part 1. General theory. J. Fluid Mech. **119** (1982), 379–408.

[5] Batchelor, G.K.; Janse van Rensburg, R.W.: Structure formation in bidisperse sedimentation. J. Fluid Mech. **166** (1986), 379–407.

[6] Batchelor, G.K.; Wen, C.S.: Sedimentation in a dilute polydisperse system of interacting spheres. Part 2. Numerical results. J. Fluid Mech. **124** (1982), 495–528.

[7] Bell, J.B.; Trangenstein, J.A.; Shubin, G.R.: Conservation laws of mixed type describing three-phase flow in porous media. SIAM J. Appl. Math. **46** (1986), 1000–1017.

[8] Biesheuvel, P.M.: Comments on "A generalized empirical description for particle slip velocities in liquid fluidized beds" by K.P. Galvin, S. Pratten and G. Nguyen Tran Lam [Chemical Engineering Science 54 (1999) 1045–1052]. Chem. Eng. Sci. **55** (2000), 1945–1947.

[9] Biesheuvel, P.M.: Particle segregation during pressure filtration for cast formation. Chem. Eng. Sci. **55** (2000), 2595–2606.

[10] Biesheuvel, P.M.; Verweij, H.: Calculation of the composition profile of a functionally graded material produced by centrifugal casting. J. Amer. Ceram. Soc. **83** (2000), 743–749.

[11] Biesheuvel, P.M.; Verweij, H.; Breedveld, V.: Evaluation of instability criterion for bidisperse sedimentation. AIChE J. **47** (2001), 45–52.

[12] BLUM, E.H.: Statistical geometric approach to the random packing of spheres. Doctoral Thesis, Dept. of Chemical Engineering, Princeton University, 1964.
[13] BRADY, J.F.; BOSSIS, G.: Stokesian dynamics. Ann. Rev. Fluid Mech. **20** (1988), 111–157.
[14] BRONSTEIN, I.N.; SEMENDJAJEW, K.A.: Taschenbuch der Mathematik. Verlag Harri Deutsch, Thun/Frankfurt am Main, 23rd edition, 1987.
[15] BÜRGER, R.: Phenomenological foundation and mathematical theory of sedimentation-consolidation processes. Chem. Eng. J. **80** (2000), 177–188.
[16] BÜRGER, R.; CONCHA, F.: Settling velocities of particulate systems: 12. Batch centrifugation of flocculated suspensions. Int. J. Mineral Process., to appear.
[17] BÜRGER, R.; CONCHA, F.; FJELDE, K.-K.; KARLSEN, K.H.: Numerical simulation of the settling of polydisperse suspensions of spheres. Powder Technol. **113** (2000), 30–54.
[18] BÜRGER, R.; FJELDE, K.-K.; HÖFLER, K.; KARLSEN, K.H.: Central difference solutions of the kinematic model of settling of polydisperse suspensions and three-dimensional particle-scale simulations. J. Eng. Math., to appear.
[19] BÜRGER, R.; WENDLAND, W.L.; CONCHA, F.: Model equations for gravitational sedimentation-consolidation processes. Z. Angew. Math. Mech. **80** (2000), 79–92.
[20] BUSTOS, M.C.; CONCHA, F.; BÜRGER, R.; TORY, E.M.: Sedimentation and Thickening, Kluwer Academic Publishers, Dordrecht, The Netherlands, 1999.
[21] CHUNG, K.L.: A course in probability theory. Academic Press, New York 1974.
[22] CONCHA, F.; BÜRGER, R.: A century of research in sedimentation and thickening. KONA Powder and Particle, submitted.
[23] DAVIS, R.H.: Effects of surface roughness on a sphere sedimenting through a dilute suspension of neutrally buoyant spheres. Phys. Fluids A **4** (1992), 2607–2619.
[24] DAVIS, R.H.: Hydrodynamic diffusion of suspended particles: a symposium. J. Fluid Mech. **310** (1996), 325–335.
[25] DAVIS, R.H.; GECOL, H.: Hindered settling function with no empirical parameters for polydisperse suspensions. AIChE J. **40** (1994), 570–575.
[26] DAVIS, R.H.; GECOL, H.: Classification of concentrated suspensions using inclined settlers. Int. J. Multiphase Flow **22** (1996), 563–574.
[27] DREW, D.A.: Mathematical modeling of two-phase flow. Ann. Rev. Fluid Mech. **15** (1983), 261–291.
[28] DRUITT, T.H.: Settling behaviour of concentrated dispersions and some volcanological applications. J. Volcanol. Geotherm. Res. **65** (1995), 27–39.
[29] FESSAS, Y.P.; WEILAND, R.H.: Convective solids settling induced by a buoyant phase. AIChE J. **27** (1981), 588–592.
[30] FESSAS, Y.P.; WEILAND, R.H.: The settling of suspensions promoted by rigid buoyant spheres. Int. J. Multiphase Flow **10** (1984), 485–507.
[31] FITT, A.D.: Mixed systems of conservation laws in industrial mathematical modelling. Surv. Math. Indust. **6** (1996), 21–53.
[32] FLOTATS, X.: Mathematical modeling of polydisperse suspensions sedimentation. Hung. J. Ind. Chem. **23** (1995), 215–221.
[33] FRID, H.: Existence and asymptotic behavior of measure-valued solutions for three-phase flow in porous media. J. Math. Anal. Appl. **196** (1995), 614–627.
[34] FRID, H.; LIU, I-S.: Oscillation waves in Riemann problems inside elliptic regions for conservation laws of mixed type. Z. Angew. Math. Phys. **46** (1995), 913–931.
[35] GALVIN, K.P.; PRATTEN, S.; NGUYEN TRAN LAM, G.: A generalized empirical description for particle slip velocities in liquid fluidized beds. Chem. Eng. Sci. **54** (1999), 1045–1052.
[36] GIDASPOW, D.: Multiphase Flow and Fluidization. Academic Press, San Diego, CA, USA, 1994.
[37] GURTIN, M.: An Introduction to Continuum Mechanics, Academic Press, San Diego, 1981.
[38] HOLDEN, H.; HOLDEN, L.; RISEBRO, N.H.: Some qualitative properties of 2×2 systems of conservation laws of mixed type. IMA Volumes in Mathematics and Its Applications **27** (1990), 67–78. Springer Verlag, New York.
[39] HÖFLER, K.: Simulation and Modeling of Mono- and Bidisperse Suspensions. Doctoral Thesis, Institute for Computer Applications, University of Stuttgart 2000.
[40] HÖFLER, K.; SCHWARZER, S.: The structure of bidisperse suspensions at low Reynolds numbers. In: SÄNDIG, A.-M.; SCHIEHLEN, W.; WENDLAND, W.L. (EDS.): Multifield Problems: State of the Art, Springer Verlag, Berlin 2000, 42–49.
[41] JACKSON, R.: The Dynamics of Fluidized Particles. Cambridge University Press, Cambridge, UK, 2000.
[42] JEFFREY, J.D.: Some basic principles in interaction calculations. In: TORY, E.M. (ED.): Sedimentation of Small Particles in a Viscous Fluid. Computational Mechanics Publications, Southampton, UK, 1996, 96–124.
[43] KEYFITZ, B.L.: A geometric theory of conservation laws which change type. Z. Angew. Math. Mech. **75** (1995), 571–581.
[44] KEYFITZ, B.L.: Mathematical properties of nonhyperbolic models for incompressible two-phase flow. Preprint.
[45] KYNCH, G.J.: A theory of sedimentation. Trans. Faraday Soc. **48** (1952), 166–176.
[46] LADD, A.J.C.: Dynamical simulations of sedimenting spheres. Phys. Fluids A **5** (1993), 299–310.

[47] LAW, H.-S.; MASLIYAH, J.H.; MACTAGGART, R.S.; NANDAKUMAR, K.: Gravity separation of bidisperse suspensions: light and heavy particle species. Chem. Eng. Sci. **42** (1987), 1527–1538.
[48] LOCKETT, M.J.; BASSOON, K.S.: Sedimentation of binary particle mixtures. Powder Technol. **24** (1979), 1–7.
[49] MARCHESIN, D.; PLOHR, B.: Wave structure in WAG recovery. SPE paper 56480.
[50] MARCHESIN D.; PLOHR, B.: Theory of three-phase flow applied to water-alternating-gas enhanced oil recovery. Proc. of the Eighth International Conference on Hyperbolic Problems, to appear.
[51] MASLIYAH, J.H.: Hindered settling in a multiple-species particle system. Chem. Eng. Sci. **34** (1979), 1166–1168.
[52] MAJDA, A.; PEGO, R.L.: Stable viscosity matrices for system of conservation laws. J. Diff. Eqns. **56** (1985), 229–262.
[53] NAKAMURA, K.; CAPES, C.E.: Vertical pneumatic conveying of binary particle mixtures. In: KEAIRNS, D.L. (ED.): Fluidization Technology, Vol. 2, Hemisphere Publ. Corp., Washington, 1976, 159–184.
[54] OSTROWSKI, A.M.: Solution of Equations in Euclidean and Banach Spaces. 3rd ed., Academic Press, New York 1973.
[55] PATWARDHAN, V.S.; TIEN, C.: Sedimentation and liquid fluidization of solid particles of different sizes and densities. Chem. Eng. Sci. **40** (1985), 1051–1060.
[56] PEGO, R.L.; SERRE, D.: Instabilities in Glimm's scheme for two systems of mixed type. SIAM J. Numer. Anal. **25** (1988), 965–988.
[57] PICKARD, D.K.; TORY, E.M.: Experimental implications of a Markov model for sedimentation. J. Math. Anal. Appl. **72** (1979), 150–176.
[58] REVAY, J.M.; HIGDON, J.J.L.: Numerical simulation of polydisperse sedimentation: equal-sized spheres. J. Fluid Mech. **243** (1992), 15–32.
[59] RICHARDSON, J.F.; ZAKI, W.N.: Sedimentation and fluidization: Part I. Trans. Instn. Chem. Engrs. (London) **32** (1954), 35–53.
[60] RUSHTON, A.; WARD, A.S.; HOLDICH, R.G.: Solid-liquid Filtration and Separation Technology. 2nd ed., Wiley-VCH, Weinheim, Germany, 2000.
[61] SARTORY, W.K.: Three-component analysis of blood sedimentation by the method of characteristics. Math. Biosci. **33** (1977), 145–165.
[62] SHIH, Y.T.; GIDASPOW, D.; WASAN, D.T.: Hydrodynamics of sedimentation of multisized particles. Powder Technol. **50** (1987), 201–215.
[63] TORY, E.M.: Stochastic sedimentation and hydrodynamic diffusion. Chem. Eng. J. **80** (2000), 81–89.
[64] TORY, E.M.; KAMEL, M.T.: Mean velocities in polydisperse suspensions. Powder Technol. **93** (1997), 199–207.
[65] TORY, E.M.; KAMEL, M.T.; CHAN MAN FONG, C.F.: Sedimentation is container-size dependent. Powder Technol. **73** (1992), 219–238.
[66] UNGARISH, M.: Hydrodynamics of Suspensions, Springer Verlag, Berlin 1993.
[67] UNGARISH, M.; GREENSPAN, H.P.: On centrifugal separation of particles of two different sizes. Int. J. Multiphase Flow **10** (1984), 133–148.
[68] VERHOEVEN, J.: Prediction of Batch Settling Behavior. B. Eng. Thesis, Dept. of Chemical Engineering, McMaster University, Hamilton, Ontario, Canada, 1963.
[69] WACHOLDER, E.; SATHER, N.F.: The hydrodynamic interaction of two unequal spheres moving under gravity through quiescent viscous fluid. J. Fluid Mech. **65** (1974), 417–437.
[70] WALLIS, G.B.: One-Dimensional Two-Phase Flow. McGraw-Hill, Inc., New York, 1969.
[71] WEILAND, R.H.; FESSAS, Y.P.; RAMARAO, B.V.: On instabilities arising during sedimentation of two-component mixtures mixtures of solids. J. Fluid Mech. **142** (1984), 383–389.
[72] YAN, Y.; MASLIYAH, J.H.: Sedimentation of solid particles in oil-in-water emulsions. Int. J. Multiphase Flow **19** (1993), 875–886.
[73] ZIMMELS, Y.: Theory of density separation of particulate systems. Powder Technol. **43** (1985), 127–139.